Geomechanics and Engineering, *Vol. 39, No. 5 (2024) 425-439*
https://doi.org/10.12989/gae.2024.39.5.425

Vibration/bending analysis of waist twisting disc with three-layer circular magnetic porous micro-plate in sports equipments during exercise

Defang Chen[1], Weiwei Wang*[1], H. Elhosiny Ali[2], Amjad S. Qazaq[3] and Minghui Long[4]

[1]*College of Sports and Health, Nanchang Institute of Science & Technology, Nanchang 330108, Jiangxi, China*
[2]*Department of Physics, Faculty of Science, King Khalid University, P.O. Box 9004, Abha 61413, Saudi Arabia*
[3]*Department of Civil Engineering, College of Engineering in Al-Kharj, Prince Sattam Bin Abdulaziz University, Al-Kharj, 11942, Saudi Arabia*
[4]*College of management, Wuhan Donghu University, Wuhan 430072, Hubei, China*

(*Received December 7, 2023, Revised October 14, 2024, Accepted November 11, 2024*)

Abstract. In the present study, bending and free vibration analyses of a micro annular plate with piezomagnetic layers are investigated based on FSDT in the presence of magnetic field and resting on the elastic foundation. The multi-field constitutive relations are developed using modified strain gradient theory and the equilibrium governing equations of motion micro annular plate are derived using minimum of total potential energy and Hamilton's principles. One can arrive at numerical results using the semi analytical solution procedure. The Ritz method is used to obtain the results in the parametric state. The boundary conditions are applied to guess the primary functions and the minimization is used to obtain the unknown coefficients in the assumed solution. The effect of micro parameter, various geometric parameter and the foundation parameter is studied on the dynamic and static responses.

Keywords: functionally graded materials; modified strain gradient theory; piezomagnetic; ritz approach; shear deformation theory

1. Introduction

Static and frequency analyses are considered as the very important requirements and as a necessary step for design of structures and mechanical elements (Meng *et al.* 2018, 2019, 2023, 2024, Xie *et al.* 2024a). Calculation of maximum deflection and frequencies of systems/structures guides designer to reach an allowable interval for actuation (Sun *et al.* 2024, Xin *et al.* 2024, Lu 2024, Luo and Dong 2024, Zhao *et al.* 2024). This act can avoid resonance and leads to an acceptable design (Li *et al.* 2024a, b, c, 2025, Lv *et al.* 2024). Calculation of maximum deflection and natural frequency based on various theories in various scales leads to different results that encourage researchers for more investigation on new theories and new size-dependent theories (Huang *et al.*2024a, b, Han *et al.* 2022a, b, 2025).

Shear deformation theories have been proposed for two-dimensional analysis of plates and shells instead of a three-dimensional one (Ji *et al.* 2023, Lai *et al.* 2024, Gao *et al.* 2023, Guo *et al.* 2024a, Cui *et al.* 2024). To account effect of very small sizes of structures specially in nano and micro scales, some size-dependent theories have been proposed by various scientists. To investigate effect of micro scale sizes, modified strain gradient theory has been used in various works. Literature review is presented in this section with considering related works on the circular plates, modified strain gradient theory and piezomagnetic materials (Bai *et al.* 2022a, 2023, 2024a, b, c).

*Corresponding author, Ph.D.
E-mail: weiweiwang0226@163.com

Liu *et al.* (2021) developed nonlocal strain gradient theory and Mindlin plate theory to size-dependent free vibration analysis of a laminated nanoplate made of piezomagnetic materials. Hamilton's principle was used to derive governing equations of motion. The numerical results were presented in both tabular and graphical forms to investigate the effect of external electromagnetic potentials, nano-scale parameter and geometric parameters on the free vibration characteristics. They studied static bending and free vibration analyses of a circular plate made of magneto-electro-elastic materials considering surface elasticity based on Kirchhoff plate theory. Comparison of the results with and without surface impact has shown this fact that this effect plays an important role in mechanical behaviors of nano-sized structures (Zhang and Zhuang 2018a, b, 2019, Zhang and Meng 2020, Zhang 2017).

Jafarsadeghi-pournaki *et al.* (2015) studied free vibration analysis of a circular nanoplate made of magnetoelectroelastic material based on Kirchhoff plate theory and nonlocal elasticity theory. The nanoplate was subjected to applied electric and magnetic potentials. After derivation of the governing equations using Maxwell's equation and Hamilton's principle, the numerical results were derived using Galerkin method. Gradation of material properties was assumed along the radial and transverse directions, simultaneously (Wang *et al.* 2024a, b, c, Wu *et al.* 2024, Pi *et al.* 2025). Coupled-stress based formulation was included in the governing equations based on first-order shear deformation theory. Wang *et al.* (2010) developed an analytical method for magneto-electro-elastic analysis of transversely isotropic axisymmetric circular plate with simply-supported boundary conditions. Solution

ISSN: 2005-307X (Print), 2092-6219 (Online)

of the governing equations was performed using the finite Hankel transform and propagating matrix methods. Prasad *et al.* (2006) studied analytical solution of a piezoelectric composite circular plate subjected to mechanical and electrical loads based on classical laminated plate theory. The main aim of this paper was computation of static transverse deflection in terms of pressure loads and applied voltage. Li *et al.* (2014) studied free vibration analysis of a laminated circular plate made of magneto-electro-elastic materials based on an axial symmetric analysis. The solution of the problem was developed based on Caylay-Hamilton and the transfer matrix method to investigate effect of significant parameters such as thickness to radius ratio, and some other geometric parameters.

Li *et al.* (2021) improved the previous analysis with accounting the nonlinear terms in the circular plate geometry.

A combination of modified strain gradient theory in conjunction with Kirchhoff plate theory were studied for finite element analysis of composite microplate by Kandaz and Dal (2021). Modified strain theory was employed for analysis of a micro plate enriched by graphene nanoplatelets subjected to thermal and mechanical loads by Arefi *et al.* (2019a). The thermal and mechanical buckling loads were estimated with changes of various micro scale parameters of the graphene nanoplatelets. A micro cantilever beam model was extended by Korayem *et al.* (2013) for investigating sensor/actuator applications of micro structures. Sadeghzadeh and Kabiri (2017) extended the previous micro scale dependent analyses for the piezoelectric cantilever beams with accounting the nonlinear geometric terms. Isogeometric-based analysis of a functionally graded plate was studied by Thai et al (2017). Kirchhoff–Love plate theory was extended for deformation analysis of micro-plate using the strain gradient terms in Cartesian coordinate system.

2. Formulation

Free vibration and bending analyses of a three-layered circular plate are studied in this paper. The kinematic relations are developed using first-order shear deformation theory (Chen *et al*. 2024, Fan *et al.* 2024a, b, Bai *et al.* 2020, Xiao *et al.* 2022):

u_1, u_2, u_3	Displacement field components
U, W	Radial and transverse displacement
r, z	Coordinate system components
$\varepsilon_{ij}, \sigma_{ij}$	Strain and stress components
E, ν, ρ	Young's modulus, Poisson's ratio and density
$V_f(z)$	volume fraction
T, U_S, V	kinetic energy, potential energy and energy due to external works
$\gamma_i, \chi_{ij}^{(s)}, \eta_{ijk}^{(1)}$	Modified strain gradient terms
$p_i, m_{ij}^{(s)}, \tau_{ijk}^{(1)}$	Modified strain gradient higher order stress terms
λ, μ	Lame's coefficient
l_0, l_1, l_2	Micro scale parameters
H_i, φ_H	Magnetic field component and magnetic potential
Q_{ij}, q_{ij}, μ_{ij}	elastic, piezomagnetic and magnetic coefficients
B_i	Magnetic induction components
$K_w, K_{G\zeta}, K_{G\eta}$	Winkler's and Pasternak's coefficients
ζ, η, δ	Foundation directions and angle
C_i, D_i, N_i, M_i	unknown amplitudes in the Ritz method
K, M	Stiffness and mass matrices
ω	Natural frequency
h, R	Thickness and radius

Based on this theory, the radial and transverse displacements are presented as (Sun *et al*. 2024, Luo *et al.* 2024a, b, Bao *et al.* 2025, Yu *et al.* (2021)

$$\begin{cases} u_1(r,t,z) = U(r,t) + z\psi(r,t) \\ u_2(r,t,z) = 0 \\ u_3(r,t,z) = W(r,t) \end{cases} \tag{1}$$

The strain components are derived using $\varepsilon_{ij} = \frac{1}{2}(U_{i,j} + U_{j,i})$ as follows (Xu *et al.* 2023, Yan *et al*. 2024, Ren *et al*. 2024, Shi *et al*. 2024, Song *et al*. 2024a)

$$\begin{cases} \varepsilon_r = \dfrac{\partial U(r,t)}{\partial r} + z\dfrac{\partial \psi(r,t)}{\partial r} \\ \varepsilon_\theta = \dfrac{U(r,t)}{r} + z\dfrac{\psi(r,t)}{r} \\ \varepsilon_{rz} = \dfrac{1}{2}(\psi(r,t) + \dfrac{\partial W(r,t)}{\partial r}) \end{cases} \tag{2}$$

The structural elements are depicted in Fig. 1 where a core and two smart layers are assumed (Zhang *et al*. 2014, 2015, 2018, 2020, 2023a). The core is assumed made from functionally graded materials in which the material properties are graded along the thickness direction based on the following relations (Zhang *et al*. 2021a, b, 2022a, b; 2024 a)

$$E(z) = (E_c - E_m)V_f(z) + E_m \tag{3.1}$$

$$\upsilon(z) = (\upsilon_c - \upsilon_m)V_f(z) + \upsilon_m \tag{3.2}$$

$$\rho(z) = (\rho_c - \rho_m)V_f(z) + \rho_m \tag{3.3}$$

In which the metal and ceramic is assumed for composition (Zhang *et al.* 2024b, c, d, Xie *et al.* 2024b).

The Hamilton's principle using an extended version of strain, kinetic and external energies is derived as (Sun *et al.* 2023, Sarvesh *et al.* 2023, Asadzadeh Khoshemehr and Bahadori 2023, Shin 2023, Jaber *et al*. 2023)

$$T = \frac{1}{2}\int_{r_i}^{r_o}\int_{-\frac{h}{2}}^{\frac{h}{2}} \rho(z)\left[\left(\frac{\partial u_1(r,z,t)}{\partial t}\right)^2 + \left(\frac{\partial u_3(r,z,t)}{\partial t}\right)^2\right] r dz\, dr \tag{4}$$

Substitution of displacement field into kinetic energy yields final form of it as follows (Arefi and Rahimi 2010, Arefi *et al*. 2012, 2016, 2018, 2020, 2022, Arefi 2016, 2018, Arefi and Zenkour 2016, Arefi and Bidgoli 2019, Bidgoli and Arefi 2022, 2023a, b, c, d, Adab *et al*. 2022, Zhang *et al.* 2023 b)

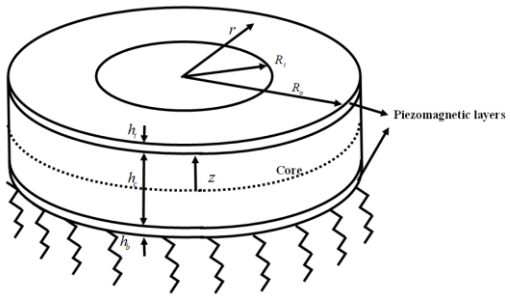

Fig. 1 The schematic figure of sandwich circular model

$$T=\frac{1}{2}\int_{r_i}^{r_o}\begin{bmatrix} I_1(\frac{\partial U(r,t)}{\partial t})^2+2I_2\frac{\partial U(r,t)}{\partial t}\frac{\partial \psi(r,t)}{\partial t} \\ +I_3(\frac{\partial \psi(r,t)}{\partial t})^2+I_1(\frac{\partial W(r,t)}{\partial t})^2 \end{bmatrix} rdr \tag{5}$$

In which the inertia constants $I_i(i=1,2,3)$ are defined as

$$\{I_1,I_2,I_3\}=\int_{-\frac{h}{2}}^{\frac{h}{2}}\rho(z)\{1,z,z^2\}dz \tag{6}$$

Potential energy is defined in the presence of magnetic potential with considering micro length scale effect associated with modified strain gradient theory as follows (Arefi and Zenkour 2017a, b, c, Arefi *et al.* 2019a, b, c)

$$U_S=\frac{1}{2}\int_{r_i}^{r_o}\int_{-\frac{h}{2}}^{\frac{h}{2}}\begin{pmatrix} \sigma_{ij}\varepsilon_{ij}+p_i\gamma_i+m_{ij}^{(s)}\chi_{ij}^{(s)} \\ +\tau_{ijk}^{(1)}\eta_{ijk}^{(1)}-B_i H_i \end{pmatrix} rdz\,dr \tag{7}$$

In which the non-classical term γ_i is defined as follows

$$\gamma_i=\varepsilon_{mm,i} \tag{8}$$

$$\begin{aligned}\gamma_r&=\frac{\partial^2U(r,t)}{\partial r^2}+\frac{1}{r}\frac{\partial U(r,t)}{\partial r}-\frac{U(r,t)}{r^2}\\ &+z\left(\frac{\partial^2\psi(r,t)}{\partial r^2}+\frac{1}{r}\frac{\partial\psi(r,t)}{\partial r}-\frac{\psi(r,t)}{r^2}\right)\\ \gamma_z&=\frac{\partial\psi(r,t)}{\partial r}+\frac{\psi(r,t)}{r}\end{aligned} \tag{9}$$

Furthermore, the non-classical term $\chi_{ij}^{(s)}$ is defined as follows (Mohammad-Rezaei Bidgoli and Arefi 2021, Thai *et al.* 2017, Li *et al.* 2014, 2021, Zhou *et al*. 2023, Kandaz *et al.* 2021)

$$\chi_{ij}^{(s)}=\frac{1}{2}(\Theta_{i,j}+\Theta_{j,i}) \tag{10}$$

$$\Theta_i=\frac{1}{2}(curl(u))_{,i} \tag{11}$$

$$\begin{aligned}\Theta_\theta&=\frac{1}{2}(\psi(r,t)-\frac{\partial W(r,t)}{\partial r})\\ \chi_{r\theta}^{(s)}&=\frac{1}{4}\begin{bmatrix}\frac{\partial\psi(r,t)}{\partial r}-\frac{\partial^2W(r,t)}{\partial r^2}\\ +\frac{1}{r}(\frac{\partial W(r,t)}{\partial r}-\psi(r,t))\end{bmatrix}\end{aligned} \tag{12}$$

Furthermore, the non-classical term $\eta_{ijk}^{(1)}$ is defined as follows (Mohammad-Rezaei Bidgoli and Arefi 2021, Arefi *et al.* 2019c, Thai *et al.* 2017, Li *et al*. 2014, 2021, Zhou *et al.* 2023, Kandaz *et al*. 2021):

$$\begin{aligned}\eta_{ijk}^{(1)}&=\frac{1}{3}(\varepsilon_{jk,i}+\varepsilon_{ki,j}+\varepsilon_{ij,k})\\ &-\frac{1}{15}\begin{bmatrix}\delta_{ij}(\varepsilon_{mm,k}+2\varepsilon_{mk,m})\\ +\delta_{jk}(\varepsilon_{mm,i}+2\varepsilon_{mi,m})\\ +\delta_{ki}(\varepsilon_{mm,j}+2\varepsilon_{mj,m})\end{bmatrix}\end{aligned} \tag{13}$$

In which the non-zero terms are developed in Appendix. Furthermore, the stress components $\sigma_{ij}=\lambda\varepsilon_{kk}\delta_{ij}+2\mu\varepsilon_{ij}$ are defined as follows

$$\begin{aligned}\sigma_r&=(\lambda(z)+2\mu(z))(\frac{\partial U(r,t)}{\partial r}+z\frac{\partial\psi(r,t)}{\partial r})\\ &+\frac{\lambda(z)}{r}(U(r,t)+z\psi(r,t))\\ \sigma_\theta&=\frac{\lambda(z)+2\mu(z)}{r}(U(r,t)+z\psi(r,t))\\ &+\lambda(\frac{\partial U(r,t)}{\partial r}+z\frac{\partial\psi(r,t)}{\partial r})\\ \sigma_{rz}&=\mu(z)(\psi(r,t)+\frac{\partial W(r,t)}{\partial r})\end{aligned} \tag{14}$$

And finally, all non-classical terms are defined as follows

$$\begin{cases}P_i=2\mu l_0^2\gamma_i\\ m_{ij}^{(s)}=2\mu l_2^2\chi_{ij}^{(s)}\\ \tau_{ijk}^{(1)}=2\mu l_1^2\eta_{ijk}^{(1)}\end{cases} \tag{15}$$

In which λ, μ are stiffness coefficients that are defined in terms of material properties as follows

$$\begin{cases}\lambda(z)=\frac{E(z)\upsilon}{1-\upsilon^2}\\ \mu(z)=\frac{E(z)}{2(1+\upsilon)}\end{cases} \tag{16}$$

The magnetic field is obtained using definition of magnetic potential as follows

$$\begin{cases}H_r=-\frac{\partial\varphi_H(\mathrm{r},\theta,z,t)}{\partial r}\\ H_\theta=-\frac{1}{R+z}\frac{\partial\varphi_H(\mathrm{r},\theta,z,t)}{\partial\theta}\\ H_z=-\frac{\partial\varphi_H(\mathrm{r},\theta,z,t)}{\partial z}\end{cases} \tag{17}$$

In which $\varphi_H(x,\theta,z,t)$ is magnetic potential. It is defined as

$$\varphi_H=-\cos(\frac{\pi z}{h_j})\psi_H+2\frac{z}{h_j}V_H \tag{18}$$

The behavior relations are

$$\begin{Bmatrix}\sigma_r\\ \sigma_\theta\\ \sigma_{rz}\end{Bmatrix}=\begin{bmatrix}Q_{11} & Q_{12} & 0\\ Q_{12} & Q_{22} & 0\\ 0 & 0 & Q_{55}\end{bmatrix}\begin{Bmatrix}\varepsilon_r\\ \varepsilon_\theta\\ \varepsilon_{rz}\end{Bmatrix} -\begin{bmatrix}0 & 0 & q_{31}\\ 0 & 0 & q_{32}\\ q_{15} & 0 & 0\end{bmatrix}\begin{Bmatrix}H_r\\ H_\theta\\ H_z\end{Bmatrix} \tag{19}$$

$$\begin{Bmatrix}B_r\\ B_\theta\\ B_z\end{Bmatrix}=\begin{bmatrix}0 & 0 & q_{15}\\ 0 & 0 & 0\\ q_{31} & q_{32} & 0\end{bmatrix}\begin{Bmatrix}\varepsilon_r\\ \varepsilon_\theta\\ \varepsilon_{rz}\end{Bmatrix} +\begin{bmatrix}\mu_{11} & 0 & 0\\ 0 & \mu_{22} & 0\\ 0 & 0 & \mu_{33}\end{bmatrix}\begin{Bmatrix}H_r\\ H_\theta\\ H_z\end{Bmatrix} \tag{20}$$

Strain energy is extended as

$$US=\frac{1}{2}\int_{r_i}^{r_o}\begin{bmatrix}N_r\dfrac{\partial U(r,t)}{\partial r}+M_r\dfrac{\partial\psi(r,t)}{\partial r}+\dfrac{N_\theta}{r}U(r,t)+\dfrac{M_\theta}{r}\psi(r,t)\\ +Q(\psi(r,t)+\dfrac{\partial W(r,t)}{\partial r})+P_r(\dfrac{\partial^2U(r,t)}{\partial r^2}+\dfrac{1}{r}\dfrac{\partial U(r,t)}{\partial r}-\dfrac{U(r,t)}{r^2})\\ +M_r^s(\dfrac{\partial^2\psi(r,t)}{\partial r^2}+\dfrac{1}{r}\dfrac{\partial\psi(r,t)}{\partial r}-\dfrac{\psi(r,t)}{r^2})+P_s(\dfrac{\partial\psi(r,t)}{\partial r}+\dfrac{\psi(r,t)}{r})\end{bmatrix}rdr$$
$$+\frac{1}{2}\int_{r_i}^{r_o}\begin{bmatrix}+\dfrac{T_{rrr}}{5}\left(2\dfrac{\partial^2u(r,t)}{\partial r^2}-\dfrac{1}{r}\dfrac{\partial u(r,t)}{\partial r}+\dfrac{u(r,t)}{r^2}\right)+\dfrac{M_{rrr}}{5}\left(2\dfrac{\partial^2\psi(r,t)}{\partial r^2}-\dfrac{1}{r}\dfrac{\partial\psi(r,t)}{\partial r}+\dfrac{\psi(r,t)}{r^2}\right)\\ -\dfrac{T_{\theta\theta\theta}}{5}\left(\dfrac{\partial^2w(r,t)}{\partial r^2}+2\dfrac{\partial\psi(r,t)}{\partial r}+\dfrac{\psi(r,t)}{r}\right)+\dfrac{T_{\theta\theta\theta}}{5}\left(4\dfrac{\partial^2w(r,t)}{\partial r^2}+8\dfrac{\partial\psi(r,t)}{\partial r}-\dfrac{\psi(r,t)}{r}\right)\\ -\dfrac{T_{\theta\theta\theta}}{5}\left(\dfrac{\partial^2w(r,t)}{\partial r^2}+2\dfrac{\partial\psi(r,t)}{\partial r}-4\dfrac{\psi(r,t)}{r}\right)+\dfrac{T_{rrr}}{5}\left(-3\dfrac{\partial^2u(r,t)}{\partial r^2}-\dfrac{1}{r}\dfrac{\partial u(r,t)}{\partial r}+\dfrac{u(r,t)}{r^2}\right)\\ +\dfrac{M_{\theta\theta\theta}}{5}\left(-3\dfrac{\partial^2\psi(r,t)}{\partial r^2}-\dfrac{1}{r}\dfrac{\partial\psi(r,t)}{\partial r}+\dfrac{\psi(r,t)}{r^2}\right)+\dfrac{T_{\theta\theta\theta}}{5}\left(-3\dfrac{\partial^2u(r,t)}{\partial r^2}+\dfrac{4}{r}\dfrac{\partial u(r,t)}{\partial r}-\dfrac{4u(r,t)}{r^2}\right)\\ +\dfrac{M_{\theta\theta\theta}}{15}\left(-3\dfrac{\partial^2\psi(r,t)}{\partial r^2}+\dfrac{4}{r}\dfrac{\partial\psi(r,t)}{\partial r}-\dfrac{4\psi(r,t)}{r^2}\right)+X_{11}\psi^2(r,t)-X_{11}(\dfrac{\partial\psi_H(r,t)}{\partial r})^2\\ +\dfrac{J_{r\theta\theta}}{2}\left(\dfrac{\partial\psi(r,t)}{\partial r}-\dfrac{\partial^2w(r,t)}{\partial r^2}+\dfrac{1}{r}\dfrac{\partial w(r,t)}{\partial r}-\dfrac{\psi(r,t)}{r}\right)+E_{12}\dfrac{u(r,t)}{r}\psi_H(r,t)+E_{12}(\dfrac{\partial w(r,t)}{\partial r}\\ +\psi(r,t))+E_{211}\dfrac{\partial u(r,t)}{\partial r}\psi_H(r,t)+E_{1111}\dfrac{\partial\psi(r,t)}{\partial r}\psi_H(r,t)+E_{1212}\dfrac{\psi(r,t)}{r}\psi_H(r,t)\end{bmatrix}rdr \tag{21}$$

The external work $F=K_W W(r,t)-(K_{G\xi}\cos^2\delta+K_{G\eta}sin^2\delta)\dfrac{\partial^2 W(r,t)}{\partial r^2}$ is assumed for computation of the external work.

$$V=\frac{1}{2}\int_A\begin{bmatrix}F-K_w W(r,t)\\ +(K_{G\xi}\cos^2\delta+K_{G\eta}sin^2\delta)\dfrac{\partial^2 W(r,t)}{\partial r^2}\end{bmatrix}W(r,t)dA \tag{22}$$

3. Solution

The Ritz method is applied for solution of the governing equations in order to apply following boundary conditions

$$\begin{cases}W(r=r_i)=0\\ \left.\dfrac{\partial W}{\partial r}\right|_{r=r_i}=0\end{cases}\square;\quad\begin{cases}W(r=r_o)=0\\ \left.\dfrac{\partial W}{\partial r}\right|_{r=r_o}=0\end{cases} \tag{23}$$

Accordingly, the unknown functions are assumed as

$$\begin{aligned}U(r,t)&=(r^2-a^2)^2(r^2-b^2)^2\\ &(C_1r^3+C_2r^2+C_3r+C_4)e^{i\omega t}\\ \psi(r,t)&=(r^2-a^2)^2(r^2-b^2)^2\\ &(C_5r^3+C_6r^2+C_7r+C_8)e^{i\omega t}\\ W(r,t)&=(r^2-a^2)^2(r^2-b^2)^2\\ &(C_9r^3+C_{10}r^2+C_{11}r+C_{12})e^{i\omega t}\\ \psi_H(r,t)&=(r^2-a^2)^2(r^2-b^2)^2\\ &(C_{13}r^3+C_{14}r^2+C_{15}r+C_{16})e^{i\omega t}\end{aligned} \tag{24}$$

The Ritz method is used to derive governing equations as follows (Bai *et al*. 2022b, Chen *et al*. 2022, Dai *et al*. 2021, 2023, Huang *et al*. 2024 c, Guo *et al*. 2024b, Gu *et al*. 2023, Huo *et al*. 2021, Liang *et al*. 2024, Li *et al*. 2022, 2024d, Lu *et al*. 2023, Liu *et al*. 2022, Jin *et al*. 2024, Ge *et al*. 2023)

$$\frac{\partial\prod}{\partial C_j}=\frac{\partial}{\partial C_j}(T-U_s-V)=0 \tag{25}$$

$$\begin{bmatrix}K_{11}-\omega^2M_{11} & K_{12} & \cdots & \cdots & \cdots & K_{1j}\\ K_{21} & K_{22}-\omega^2M_{22} & \cdots & \cdots & \cdots & K_{2j}\\ & & K_{33}-\omega^2M_{33} & \cdots & \cdots & \cdots\\ & & & \cdots & \cdots & \cdots\\ & Sym & & & \cdots & \cdots\\ & & & & & K_{jj}-\omega^2M_{jj}\end{bmatrix}\begin{Bmatrix}C_1\\ C_2\\ \cdots\\ \cdots\\ \cdots\\ C_j\end{Bmatrix}=\begin{Bmatrix}0\\ 0\\ \cdots\\ \cdots\\ \cdots\\ 0\end{Bmatrix} \tag{26}$$

$$\left|K-M\omega^2\right|=0 \tag{27}$$

$$\begin{bmatrix}K_{11} & K_{12} & \cdots & \cdots & \cdots & K_{116}\\ & K_{22} & \cdots & \cdots & \cdots & K16\\ & & K_{33} & \cdots & \cdots & \cdots\\ & & & \cdots & \cdots & \cdots\\ & Sym & & & \cdots & \cdots\\ & & & & & K_{1616}\end{bmatrix}\begin{Bmatrix}C_1\\ C_2\\ \cdots\\ \cdots\\ \cdots\\ C_{16}\end{Bmatrix}=\begin{Bmatrix}F_1\\ F_2\\ \cdots\\ \cdots\\ \cdots\\ F_{16}\end{Bmatrix} \tag{28}$$

$$\{C_1\quad C_2\quad\cdots\quad\cdots\quad\cdots\quad C_{16}\}^T=[K]^{-1}\times\{F\} \tag{29}$$

4. Numerical results and discussion

Numerical results including natural frequencies and bending results are calculated in terms of significant parameters such as geometric and material characteristics of composed materials (Wang *et al.* 2023a, b, 2024f, Fu *et al.* 2023). A comparative study is presented for validation of numerical results and solution procedure. Material properties of constituent materials are assumed as (Zhang *et al.* 2023d, e, 2024g, Li 2024 e, f):

$$E_{Sic}=427MPa, E_{Al}=70MPa, \upsilon_{Sic}=0.17, \upsilon_{Al}=0.3,$$
$$\rho_{Sic}=3100\,kg/m^3, \rho_{Al}=2702\,kg/m^3$$

Upper and lower layers are made from $CoFe_2O_4$. The material properties of $CoFe_2O_4$ are expressed as

Table 1 Natural frequencies in terms of thickness to micro length scale dimensionless ratio h/l based on various size-dependent theories

h/l	Classical Theory	Modified Couple Stress Theory	Modified Strain Gradient Theory
2	4858.22	21125.34	20756.49
2.2	4858.22	19922.89	19575.04
2.4	4858.22	18720.44	18393.58
2.6	4858.22	17517.99	17212.13
2.8	4858.22	16315.54	16030.67
3	4858.22	15025.94	14763.59
3.2	4858.22	14645.70	14389.99
3.4	4858.22	14265.46	14016.39
3.6	4858.22	13885.22	13642.78
3.8	4858.22	13504.98	13269.18
4	4858.22	13125.68	12896.51
4.2	4858.22	12564.98	12345.59
4.4	4858.22	12004.27	11794.68
4.6	4858.22	11443.57	11243.76
4.8	4858.22	10882.86	10692.85
5	4858.22	10354.58	10173.79
5.2	4858.22	10154.93	9977.62
5.4	4858.22	9955.28	9857.72
5.6	4858.22	9755.63	9660.02
5.8	4858.22	9555.98	9462.33
6	4858.22	9325.25	9233.86
6.2	4858.22	9043.20	8954.58
6.4	4858.22	8761.15	8675.29
6.6	4858.22	8479.10	8396.00
6.8	4858.22	8197.05	8116.72
7	4858.22	7982.74	7904.51
7.2	4858.22	7852.49	7775.54
7.4	4858.22	7722.24	7646.56
7.6	4858.22	7591.99	7517.59
7.8	4858.22	7461.74	7388.61
8	4858.22	7326.72	7254.92
8.2	4858.22	7196.47	7125.94
8.4	4858.22	7066.22	6996.97
8.6	4858.22	6935.97	6868.00
8.8	4858.22	6805.72	6739.02
9	4858.22	6825.26	6758.37
9.2	4858.22	6685.61	6620.09
9.4	4858.22	6545.96	6481.81
9.6	4858.22	6406.31	6343.53
9.8	4858.22	6266.66	6205.25
10	4858.22	6127.01	6066.97

$Q_{11}=286MPa, Q_{12}=173MPa, Q_{55}=45.3MPa, \rho=5300\,kg/m^3$,
$q_{31}=580.3\,\mathrm{N/Am}, q_{32}=580.3\,\mathrm{N/Am}, q_{15}=550\,\mathrm{N/Am}$,
$\mu_{11}=-590\times10^{-6}\,Ns^2/C^2$, $\mu_{33}=157\times10^{-6}\,Ns^2/C^2$

Table 2 Natural frequencies in terms of outer radius to thickness ratio r/h based on various size-dependent theories

r/h	h/l=1	h/l=2	h/l=4	h/l=8
1	34897.25	29013.57	22431.95	17947.66
1.1	34485.15	28670.95	22167.05	17735.71
1.2	34073.05	28328.33	21902.16	17523.77
1.3	33660.95	27985.71	21637.26	17311.83
1.4	33248.85	27643.09	21372.36	17099.88
1.5	32836.22	27300.03	21107.12	16887.67
1.6	32476.06	27000.6	20875.61	16702.44
1.7	32115.90	26701.16	20644.1	16517.21
1.8	31755.74	26401.72	20412.59	16331.98
1.9	31395.58	26102.29	20181.08	16146.75
2	31025.36	25794.48	19943.1	15956.34
2.1	30665.17	25495.02	19711.57	15771.1
2.2	30304.98	25195.56	19480.04	15585.85
2.3	29944.79	24896.1	19248.51	15400.61
2.4	29584.60	24596.64	19016.98	15215.36
2.5	30025.25	24962.99	19300.23	15441.99
2.6	29805.25	24780.08	19158.81	15328.84
2.7	29585.25	24597.18	19017.4	15215.69
2.8	29365.25	24414.27	18875.98	15102.55
2.9	29145.25	24231.36	18734.57	14989.4
3	28925.25	24048.45	18593.15	14876.26
3.1	28785.25	23932.06	18503.16	14804.25
3.2	28645.25	23815.66	18413.17	14732.25
3.3	28505.25	23699.26	18323.17	14660.25
3.4	28365.25	23582.87	18233.18	14588.25
3.5	28225.25	23466.47	18143.19	14516.25
3.6	28115.25	23375.02	18072.48	14459.67
3.7	28005.25	23283.56	18001.77	14403.1
3.8	27895.25	23192.11	17931.07	14346.53
3.9	27785.25	23100.66	17860.36	14289.95
4	27675.25	23009.2	17789.65	14233.38
4.1	27605.25	22951	17744.65	14197.38
4.2	27535.25	22892.81	17699.66	14161.38
4.3	27465.25	22834.61	17654.66	14125.38
4.4	27395.25	22776.41	17609.67	14089.38
4.5	27325.25	22718.21	17564.67	14053.38
4.6	27295.25	22693.27	17545.39	14037.95
4.7	27265.25	22668.33	17526.1	14022.52
4.8	27235.25	22643.39	17506.82	14007.09
4.9	27205.25	22618.44	17487.53	13991.66
5	27175.25	22593.5	17468.25	13976.23
5.1	27145.25	22568.56	17448.97	13960.8
5.2	27115.25	22543.62	17429.68	13945.37
5.3	27085.25	22518.68	17410.4	13929.94
5.4	27055.25	22493.73	17391.11	13914.52
5.5	27025.25	22468.79	17371.83	13899.09
5.6	26995.25	22443.85	17352.55	13883.66
5.7	26965.25	22418.91	17333.26	13868.23
5.8	26935.25	22393.97	17313.98	13852.8
5.9	26905.25	22369.02	17294.69	13837.37
6	26875.25	22344.08	17275.41	13821.94

Table 3 Variation of frequencies in terms of ht/h for various n

ht/h	n=1	n=2	n=3	n=4
0.020	22125.87	20206.45	19473.42	18641.49
0.024	28491.81	26020.14	25076.21	24004.92
0.028	34857.74	31833.83	30679.00	29368.35
0.032	41223.68	37647.53	36281.78	34731.77
0.036	47589.62	43461.22	41884.57	40095.20
0.040	53955.55	49274.91	47487.36	45458.63
0.044	60321.49	55088.60	53090.15	50822.06
0.048	66687.43	60902.29	58692.94	56185.49
0.052	73053.36	66715.98	64295.72	61548.92
0.056	79419.30	72529.67	69898.51	66912.35
0.060	85785.24	78343.37	75501.30	72275.78
0.064	92151.17	84157.06	81104.09	77639.21
0.068	98517.11	89970.75	86706.88	83002.63
0.072	104883.04	95784.44	92309.67	88366.06
0.076	111248.98	101598.13	97912.45	93729.49
0.080	117614.92	107411.82	103515.24	99092.92
0.084	123980.85	113225.51	109118.03	104456.35
0.088	130346.79	119039.21	114720.82	109819.78
0.092	136712.73	124852.90	120323.61	115183.21
0.096	143078.66	130666.59	125926.39	120546.64
0.100	149444.60	136480.28	131529.18	125910.06
0.104	155810.54	142293.97	137131.97	131273.49
0.108	162176.47	148107.66	142734.76	136636.92
0.112	168542.41	153921.36	148337.55	142000.35
0.116	174908.35	159735.05	153940.33	147363.78
0.120	181274.28	165548.74	159543.12	152727.21
0.124	187640.22	171362.43	165145.91	158090.64
0.128	194006.16	177176.12	170748.70	163454.07
0.132	200372.09	182989.81	176351.49	168817.49
0.136	206738.03	188803.50	181954.27	174180.92
0.140	213103.97	194617.20	187557.06	179544.35
0.144	219469.90	200430.89	193159.85	184907.78
0.148	225835.84	206244.58	198762.64	190271.21
0.152	232201.77	212058.27	204365.43	195634.64
0.156	238567.71	217871.96	209968.21	200998.07
0.160	244933.65	223685.65	215571.00	206361.50
0.164	251299.58	229499.35	221173.79	211724.93
0.168	257665.52	235313.04	226776.58	217088.35
0.172	264031.46	241126.73	232379.37	222451.78
0.176	270397.39	246940.42	237982.15	227815.21
0.180	276763.33	252754.11	243584.94	233178.64
0.184	283129.27	258567.80	249187.73	238542.07
0.188	289495.20	264381.49	254790.52	243905.50
0.192	295861.14	270195.19	260393.31	249268.93
0.196	302227.08	276008.88	265996.09	254632.36
0.200	308593.01	281822.57	271598.88	259995.78

The geometric parameters are obtained from the following data

$$l=15\mu m, h=4l, h_t=h_b=0.05h,\ r_i=0.5r_o\ \ (\alpha=0.5), b=6h, K_p=0.5, K_S=\frac{\pi^2}{12}$$

and

$$K_W=2(\mathrm{TN/m^3}), K_{G\eta}=2(\mathrm{MN/m}), K_{G\xi}=2(\mathrm{MN/m}), \delta=\pi/9(rad)$$

In continuation, the main numerical results are presented in terms of significant parameters such micro length scale parameter, geometric parameters, in-homogeneous index based on various theories (Li *et al*. 2024d, e, f).

Table 4 Variation of natural frequencies in terms of n for various ht/h

n	ht/h=0.19	ht/h=0.16	ht/h=0.13	ht/h=0.10
0.0	97254.24	41352.50	21837.47	5001.79
0.5	96552.01	41053.91	21679.79	4965.67
1.0	95849.78	40755.33	21522.11	4929.55
1.5	95147.55	40456.74	21364.43	4893.44
2.0	94445.32	40158.15	21206.75	4857.32
2.5	93743.09	39859.56	21049.07	4821.21
3.0	93040.86	39560.97	20891.39	4785.09
3.5	92338.63	39262.38	20733.72	4748.98
4.0	91636.40	38963.80	20576.04	4712.86
4.5	90934.17	38665.21	20418.36	4676.74
5.0	90231.94	38366.62	20260.68	4640.63
5.5	89529.70	38068.03	20103.00	4604.51
6.0	88827.47	37769.44	19945.32	4568.40
6.5	88125.24	37470.85	19787.64	4532.28
7.0	87423.01	37172.27	19629.96	4496.17
7.5	86720.78	36873.68	19472.28	4460.05
8.0	86018.55	36575.09	19314.61	4423.93
8.5	85316.32	36276.50	19156.93	4387.82
9.0	84614.09	35977.91	18999.25	4351.70
9.5	83911.86	35679.32	18841.57	4315.59
10.0	83209.63	35380.73	18683.89	4279.47
10.5	82507.40	35082.15	18526.21	4243.36
11.0	81805.17	34783.56	18368.53	4207.24
11.5	81102.94	34484.97	18210.85	4171.12
12.0	80400.71	34186.38	18053.18	4135.01
12.5	79698.48	33887.79	17895.50	4098.89
13.0	78996.25	33589.20	17737.82	4062.78
13.5	78294.02	33290.62	17580.14	4026.66
14.0	77591.79	32992.03	17422.46	3990.55
14.5	76889.56	32693.44	17264.78	3954.43
15.0	76187.33	32394.85	17107.10	3918.31
15.5	75485.10	32096.26	16949.42	3882.20
16.0	74782.86	31797.67	16791.74	3846.08
16.5	74080.63	31499.09	16634.07	3809.97
17.0	73378.40	31200.50	16476.39	3773.85
17.5	72676.17	30901.91	16318.71	3737.74
18.0	71973.94	30603.32	16161.03	3701.62
18.5	71271.71	30304.73	16003.35	3665.50
19.0	70569.48	30006.14	15845.67	3629.39
19.5	69867.25	29707.56	15687.99	3593.27
20.0	69165.02	29408.97	15530.31	3557.16
20.5	68462.79	29110.38	15372.63	3521.04
21.0	67760.56	28811.79	15214.96	3484.93
21.5	67058.33	28513.20	15057.28	3448.81
22.0	66356.10	28214.61	14899.60	3412.69
22.5	65653.87	27916.02	14741.92	3376.58
23.0	64951.64	27617.44	14584.24	3340.46
23.5	64249.41	27318.85	14426.56	3304.35
24.0	63547.18	27020.26	14268.88	3268.23
24.5	62844.95	26721.67	14111.20	3232.12
25.0	62142.72	26423.08	13953.53	3196.00

Shown in Table 1 is variation of dimensionless natural frequencies of three-layered micro plate in terms of h/l based on three theories named as modified couple stress,

Table 5 Variation of frequencies in terms of K_w for various K_G

K_w	KG=0	KG=5000	KG=10000	KG=15000
0	221525.25	215156.40	206585.59	199928.75
500	222327.76	215935.83	207333.97	200653.02
1000	223130.26	216715.27	208082.36	201377.29
1500	223932.77	217494.70	208830.74	202101.56
2000	224735.27	218274.13	209579.12	202825.83
2500	225537.78	219053.56	210327.51	203550.10
3000	226340.28	219833.00	211075.89	204274.37
3500	227142.79	220612.43	211824.28	204998.63
4000	227945.29	221391.86	212572.66	205722.90
4500	228747.80	222171.30	213321.04	206447.17
5000	229550.30	222950.73	214069.43	207171.44
5500	230352.81	223730.16	214817.81	207895.71
6000	231155.31	224509.59	215566.20	208619.98
6500	231957.82	225289.03	216314.58	209344.25
7000	232760.32	226068.46	217062.96	210068.52
7500	233562.83	226847.89	217811.35	210792.79
8000	234365.33	227627.33	218559.73	211517.05
8500	235167.84	228406.76	219308.12	212241.32
9000	235970.34	229186.19	220056.50	212965.59
9500	236772.85	229965.63	220804.88	213689.86
10000	237575.35	230745.06	221553.27	214414.13
10500	238377.86	231524.49	222301.65	215138.40
11000	239180.36	232303.92	223050.04	215862.67
11500	239982.87	233083.36	223798.42	216586.94
12000	240785.37	233862.79	224546.80	217311.20
12500	241587.88	234642.22	225295.19	218035.47
13000	242390.38	235421.66	226043.57	218759.74
13500	243192.89	236201.09	226791.96	219484.01
14000	243995.39	236980.52	227540.34	220208.28
14500	244797.90	237759.96	228288.72	220932.55
15000	245600.40	238539.39	229037.11	221656.82
15500	246402.91	239318.82	229785.49	222381.09
16000	247205.41	240098.25	230533.88	223105.35
16500	248007.92	240877.69	231282.26	223829.62
17000	248810.42	241657.12	232030.65	224553.89
17500	249612.93	242436.55	232779.03	225278.16
18000	250415.43	243215.99	233527.41	226002.43
18500	251217.94	243995.42	234275.80	226726.70
19000	252020.44	244774.85	235024.18	227450.97
19500	252822.95	245554.29	235772.57	228175.24
20000	253625.45	246333.72	236520.95	228899.50
20500	254427.96	247113.15	237269.33	229623.77
21000	255230.46	247892.58	238017.72	230348.04
21500	256032.97	248672.02	238766.10	231072.31
22000	256835.47	249451.45	239514.49	231796.58
22500	257637.98	250230.88	240262.87	232520.85

Table 6 Variation of frequencies in terms of $K_{G\xi}$ for various values of $K_{G\eta}$

$K_{G\eta}$	$K_{G\xi}=5000$	$K_{G\xi}=10000$	$K_{G\xi}=15000$	$K_{G\xi}=20000$
0.00	160242.00	164171.13	167058.69	172396.36
0.02	160907.04	164852.48	167752.03	173111.84
0.04	161572.08	165533.83	168445.36	173827.32
0.06	162237.12	166215.17	169138.69	174542.81
0.08	162902.16	166896.52	169832.02	175258.29
0.10	163567.20	167577.87	170525.35	175973.77
0.12	164232.24	168259.21	171218.68	176689.26
0.14	164897.28	168940.56	171912.01	177404.74
0.16	165562.32	169621.91	172605.34	178120.22
0.18	166227.36	170303.25	173298.67	178835.71
0.20	166892.40	170984.60	173992.00	179551.19
0.22	167557.44	171665.95	174685.33	180266.67
0.24	168222.48	172347.30	175378.66	180982.16
0.26	168887.52	173028.64	176072.00	181697.64
0.28	169552.56	173709.99	176765.33	182413.12
0.30	170217.60	174391.34	177458.66	183128.60
0.32	170882.64	175072.68	178151.99	183844.09
0.34	171547.68	175754.03	178845.32	184559.57
0.36	172212.72	176435.38	179538.65	185275.05
0.38	172877.76	177116.72	180231.98	185990.54
0.40	173542.80	177798.07	180925.31	186706.02
0.42	174207.84	178479.42	181618.64	187421.50
0.44	174872.88	179160.76	182311.97	188136.99
0.46	175537.92	179842.11	183005.30	188852.47
0.48	176202.96	180523.46	183698.63	189567.95
0.50	176868.00	181204.80	184391.96	190283.44
0.52	177533.04	181886.15	185085.30	190998.92
0.54	178198.08	182567.50	185778.63	191714.40
0.56	178863.12	183248.84	186471.96	192429.89
0.58	179528.16	183930.19	187165.29	193145.37
0.60	180193.20	184611.54	187858.62	193860.85
0.62	180858.24	185292.88	188551.95	194576.34
0.64	181523.28	185974.23	189245.28	195291.82
0.66	182188.32	186655.58	189938.61	196007.30
0.68	182853.36	187336.92	190631.94	196722.79
0.70	183518.40	188018.27	191325.27	197438.27
0.72	184183.44	188699.62	192018.60	198153.75
0.74	184848.48	189380.96	192711.93	198869.24
0.76	185513.52	190062.31	193405.27	199584.72
0.78	186178.56	190743.66	194098.60	200300.20
0.80	186843.60	191425.01	194791.93	201015.69
0.82	187508.64	192106.35	195485.26	201731.17
0.84	188173.68	192787.70	196178.59	202446.65
0.86	188838.72	193469.05	196871.92	203162.14
0.88	189503.76	194150.39	197565.25	203877.62
0.90	190168.80	194831.74	198258.58	204593.10
0.92	190833.84	195513.09	198951.91	205308.59
0.94	191498.88	196194.43	199645.24	206024.07
0.96	192163.92	196875.78	200338.57	206739.55
0.98	192828.96	197557.13	201031.90	207455.04
1.00	193494.00	198238.47	201725.23	208170.52

modified strain gradient and classic theories (Yuan *et al.* 2024, Huang *et al.* 2022a, b, Su *et al.* 2023). the obtained results indicate that the dimensionless natural frequencies are decreased with an increase in the thickness to micro length scale dimensionless ratio h/l. A decrease in natural frequencies is observed with an enhancement in the h/l parameter. As an another important result, it is concluded that the natural frequencies predicted by modified strain gradient theory is over-calculated another two theories (Jermsittiparsert *et al.* 2020, Ma *et al.* 2023, Peng *et al.* 2023, Song *et al.* 2024b, Shi *et al.* 2022, Wang *et al.* 2023c, 2024d, e, Wu and Habibi 2022, Xiao *et al*. 2024, Yu *et al.* 2024, Yin *et al.* 2024, Zhu *et al.* 2022, Zhiqiang *et al.* 2024, Zhang *et al.* 2021c, 2023c, d, 2024e, f).

Table 7 Variation of frequencies in terms of local angle δ for various $K_{G\eta}$

δ	$K_{G\eta}=0$	$K_{G\eta}=10000$	$K_{G\eta}=20000$	$K_{G\eta}=30000$	$K_{G\eta}=40000$
0	162512.25	162512.25	162512.25	162512.25	162512.25
0.05	162391.74	162407.21	162469.21	162657.30	162777.90
0.1	162271.24	162302.16	162426.16	162802.35	163043.55
0.15	162150.73	162197.12	162383.12	162947.40	163309.20
0.2	162030.23	162092.07	162340.07	163092.45	163574.85
0.25	161909.72	161987.03	162297.03	163237.50	163840.50
0.3	161789.22	161881.98	162253.98	163382.55	164106.15
0.35	161668.71	161776.94	162210.94	163527.60	164371.80
0.4	161548.21	161671.89	162167.89	163672.65	164637.45
0.45	161427.70	161566.85	162124.85	163817.70	164903.10
0.5	161307.20	161461.80	162081.80	163962.75	165168.75
0.55	161186.69	161356.76	162038.76	164107.80	165434.40
0.6	161066.19	161251.71	161995.71	164252.85	165700.05
0.65	160945.68	161146.67	161952.67	164397.91	165965.71
0.7	160825.17	161041.62	161909.62	164542.96	166231.36
0.75	160704.67	160936.58	161866.58	164688.01	166497.01
0.8	160584.16	160831.53	161823.53	164833.06	166762.66
0.85	160463.66	160726.49	161780.49	164978.11	167028.31
0.9	160343.15	160621.44	161737.44	165123.16	167293.96
0.95	160222.65	160516.40	161694.40	165268.21	167559.61
1	160102.14	160411.35	161651.35	165413.26	167825.26
1.05	159981.64	160306.31	161608.31	165558.31	168090.91
1.1	159861.13	160201.26	161565.26	165703.36	168356.56
1.15	159740.63	160096.22	161522.22	165848.41	168622.21
1.2	159620.12	159991.17	161479.17	165993.46	168887.86
1.25	159499.62	159886.13	161436.13	166138.51	169153.51
1.3	159379.11	159781.08	161393.08	166283.56	169419.16
1.35	159258.60	159676.04	161350.04	166428.61	169684.81
1.4	159138.10	159570.99	161306.99	166573.66	169950.46
1.45	159017.59	159465.95	161263.95	166718.71	170216.11
1.5	158897.09	159360.90	161220.90	166863.76	170481.76
1.55	158776.58	159255.86	161177.86	167008.81	170747.41
1.6	158656.08	159150.81	161134.82	167153.86	171013.06
1.65	158535.57	159045.77	161091.77	167298.91	171278.71
1.7	158415.07	158940.72	161048.73	167443.96	171544.36
1.75	158294.56	158835.68	161005.68	167589.01	171810.01
1.8	158174.06	158730.63	160962.64	167734.06	172075.66
1.85	158053.55	158625.59	160919.59	167879.11	172341.31
1.9	157933.04	158520.54	160876.55	168024.17	172606.97
1.95	157812.54	158415.50	160833.50	168169.22	172872.62
2	157692.03	158310.45	160790.46	168314.27	173138.27
2.05	157571.53	158205.40	160747.41	168459.32	173403.92
2.1	157451.02	158100.36	160704.37	168604.37	173669.57
2.15	157330.52	157995.31	160661.32	168749.42	173935.22
2.2	157210.01	157890.27	160618.28	168894.47	174200.87
2.25	157089.51	157785.22	160575.23	169039.52	174466.52
2.3	156969.00	157680.18	160532.19	169184.57	174732.17
2.35	156848.50	157575.13	160489.14	169329.62	174997.82
2.4	156727.99	157470.09	160446.10	169474.67	175263.47
2.45	156607.49	157365.04	160403.05	169619.72	175529.12
2.5	156486.98	157260.00	160360.01	169764.77	175794.77

Shown in Table 2 are variation of dimensionless natural frequencies in terms of outer radius to thickness dimensionless ratio r/h for various dimensionless ratio r/h. A decrease in dimensionless natural frequencies is observed with an increase in r/h and h/l.

Table 8 Variation of deflection in terms of h/l

h/l	Classical Theory	Modified Couple Stress Theory	Modified Strain Gradient Theory
2	6.71252	6.71252	2.88253
2.2	6.71252	6.71252	2.95903
2.4	6.71252	6.71252	3.03553
2.6	6.71252	6.71252	3.11203
2.8	6.71252	6.71252	3.18853
3	6.71252	6.71252	3.26503
3.2	6.71252	6.71252	3.34153
3.4	6.71252	6.71252	3.41803
3.6	6.71252	6.71252	3.49453
3.8	6.71252	6.71252	3.57103
4	6.71252	6.71252	3.64753
4.2	6.71252	6.71252	3.72403
4.4	6.71252	6.71252	3.80053
4.6	6.71252	6.71252	3.87703
4.8	6.71252	6.71252	3.95353
5	6.71252	6.71252	4.03003
5.2	6.71252	6.71252	4.10653
5.4	6.71252	6.71252	4.18303
5.6	6.71252	6.71252	4.25953
5.8	6.71252	6.71252	4.33603
6	6.71252	6.71252	4.41253
6.2	6.71252	6.71252	4.48903
6.4	6.71252	6.71252	4.56553
6.6	6.71252	6.71252	4.64203
6.8	6.71252	6.71252	4.71853
7	6.71252	6.71252	4.79503
7.2	6.71252	6.71252	4.87153
7.4	6.71252	6.71252	4.94803
7.6	6.71252	6.71252	5.02453
7.8	6.71252	6.71252	5.10103
8	6.71252	6.71252	5.17753
8.2	6.71252	6.71252	5.25403
8.4	6.71252	6.71252	5.33053
8.6	6.71252	6.71252	5.40703
8.8	6.71252	6.71252	5.48353
9	6.71252	6.71252	5.56003
9.2	6.71252	6.71252	5.63653
9.4	6.71252	6.71252	5.71303
9.6	6.71252	6.71252	5.78953
9.8	6.71252	6.71252	5.86603
10	6.71252	6.71252	5.94253

Shown in Table 3 are variation of dimensionless natural frequencies of three-layered micro plate in terms of face-sheets thickness to core thickness ratio ht/h for various in-homogeneous index. An increase in natural frequencies is observed with an increase in face-sheets thickness to core thickness ratio ht/h due to an increase in structural stiffness. Furthermore, an increase in in-homogeneous index leads to significant decrease in structural stiffness and consequently decrease in natural frequencies.

Shown in Table 4 are variation of frequencies of in terms of n for various ht/h. A significant decrease in natural frequencies is observed with an increase in n.

Shown in Table 5 are variation of dimensionless natural frequencies in terms of K_w for various K_G. The results show an enhancement in the frequencies with an increase in both mentioned parameters.

Table 9 Variation of deflection in terms of r/h for various h/l

r/h	h/l=1	h/l=2	h/l=4	h/l=8
1	0.00000	0.00000	0.00000	0.00000
1.1	0.06508	0.10761	0.12935	0.13529
1.2	0.13016	0.21522	0.25869	0.27059
1.3	0.19524	0.32284	0.38804	0.40588
1.4	0.26032	0.43045	0.51739	0.54117
1.5	0.32540	0.53806	0.64673	0.67647
1.6	0.39048	0.64567	0.77608	0.81176
1.7	0.45556	0.75329	0.90543	0.94705
1.8	0.52064	0.86090	1.03477	1.08235
1.9	0.58572	0.96851	1.16412	1.21764
2	0.65080	1.07612	1.29347	1.35294
2.1	0.71588	1.18374	1.42281	1.48823
2.2	0.78096	1.29135	1.55216	1.62352
2.3	0.84604	1.39896	1.68150	1.75882
2.4	0.91112	1.50657	1.81085	1.89411
2.5	0.97620	1.61419	1.94020	2.02940
2.6	1.04128	1.72180	2.06954	2.16470
2.7	1.10636	1.82941	2.19889	2.29999
2.8	1.17144	1.93702	2.32824	2.43528
2.9	1.23652	2.04464	2.45758	2.57058
3	1.30160	2.15225	2.58693	2.70587
3.1	1.36668	2.25986	2.71628	2.84116
3.2	1.43176	2.36747	2.84562	2.97646
3.3	1.49684	2.47508	2.97497	3.11175
3.4	1.56192	2.58270	3.10432	3.24704
3.5	1.62700	2.69031	3.23366	3.38234
3.6	1.69208	2.79792	3.36301	3.51763
3.7	1.75716	2.90553	3.49236	3.65292
3.8	1.82224	3.01315	3.62170	3.78822
3.9	1.88732	3.12076	3.75105	3.92351
4	1.95240	3.22837	3.88040	4.05881
4.1	2.01748	3.33598	4.00974	4.19410
4.2	2.08256	3.44360	4.13909	4.32939
4.3	2.14764	3.55121	4.26843	4.46469
4.4	2.21272	3.65882	4.39778	4.59998
4.5	2.27780	3.76643	4.52713	4.73527
4.6	2.34288	3.87405	4.65647	4.87057
4.7	2.40796	3.98166	4.78582	5.00586
4.8	2.47304	4.08927	4.91517	5.14115
4.9	2.53812	4.19688	5.04451	5.27645
5	2.60320	4.30450	5.17386	5.41174
5.1	2.66828	4.41211	5.30321	5.54703
5.2	2.73336	4.51972	5.43255	5.68233
5.3	2.79844	4.62733	5.56190	5.81762
5.4	2.86352	4.73494	5.69125	5.95291
5.5	2.92860	4.84256	5.82059	6.08821
5.6	2.99368	4.95017	5.94994	6.22350
5.7	3.05876	5.05778	6.07929	6.35879
5.8	3.12384	5.16539	6.20863	6.49409
5.9	3.18892	5.27301	6.33798	6.62938
6	3.25400	5.38062	6.46733	6.76468

Table 10 Effect of n on the variation of deflection in terms of ht/h

n	ht/h=0.19	ht/h=0.16	ht/h=0.13	ht/h=0.10
0.0	13.67254	17.94576	20.31712	21.00786
0.5	13.74369	18.03914	20.42285	21.11718
1.0	13.81484	18.13253	20.52858	21.22651
1.5	13.88599	18.22592	20.63431	21.33583
2.0	13.95715	18.31931	20.74004	21.44515
2.5	14.02830	18.41270	20.84577	21.55448
3.0	14.09945	18.50609	20.95150	21.66380
3.5	14.17060	18.59948	21.05723	21.77313
4.0	14.24175	18.69287	21.16296	21.88245
4.5	14.31290	18.78626	21.26869	21.99177
5.0	14.38405	18.87965	21.37442	22.10110
5.5	14.45521	18.97304	21.48015	22.21042
6.0	14.52636	19.06642	21.58588	22.31975
6.5	14.59751	19.15981	21.69161	22.42907
7.0	14.66866	19.25320	21.79733	22.53840
7.5	14.73981	19.34659	21.90306	22.64772
8.0	14.81096	19.43998	22.00879	22.75704
8.5	14.88211	19.53337	22.11452	22.86637
9.0	14.95327	19.62676	22.22025	22.97569
9.5	15.02442	19.72015	22.32598	23.08502
10.0	15.09557	19.81354	22.43171	23.19434
10.5	15.16672	19.90693	22.53744	23.30366
11.0	15.23787	20.00031	22.64317	23.41299
11.5	15.30902	20.09370	22.74890	23.52231
12.0	15.38017	20.18709	22.85463	23.63164
12.5	15.45133	20.28048	22.96036	23.74096
13.0	15.52248	20.37387	23.06609	23.85028
13.5	15.59363	20.46726	23.17182	23.95961
14.0	15.66478	20.56065	23.27755	24.06893
14.5	15.73593	20.65404	23.38328	24.17826
15.0	15.80708	20.74743	23.48901	24.28758
15.5	15.87823	20.84082	23.59474	24.39691
16.0	15.94938	20.93421	23.70047	24.50623
16.5	16.02054	21.02759	23.80620	24.61555
17.0	16.09169	21.12098	23.91193	24.72488
17.5	16.16284	21.21437	24.01766	24.83420
18.0	16.23399	21.30776	24.12339	24.94353
18.5	16.30514	21.40115	24.22911	25.05285
19.0	16.37629	21.49454	24.33484	25.16217
19.5	16.44744	21.58793	24.44057	25.27150
20.0	16.51860	21.68132	24.54630	25.38082
20.5	16.58975	21.77471	24.65203	25.49015
21.0	16.66090	21.86810	24.75776	25.59947
21.5	16.73205	21.96149	24.86349	25.70880
22.0	16.80320	22.05487	24.96922	25.81812
22.5	16.87435	22.14826	25.07495	25.92744
23.0	16.94550	22.24165	25.18068	26.03677
23.5	17.01666	22.33504	25.28641	26.14609
24.0	17.08781	22.42843	25.39214	26.25542
24.5	17.15896	22.52182	25.49787	26.36474
25.0	17.23011	22.61521	25.60360	26.47406

Tables 6 and 7 investigates effect of spring and shear parameters of orthotropic Pasternak foundation along directions ξ and η with local angle δ on the variation of natural frequencies of microplate. Table 7 shows variation of natural frequencies of micro plate in terms of $K_{G\xi}$ for various values of $K_{G\eta}$. An increase in natural frequencies is observed with an increase in both shear parameter of foundation $K_{G\xi}$, $K_{G\eta}$.

Table 11 Variation of deflection in terms of δ for various $K_{G\eta}$

δ	$K_{G\eta}=40000$	$K_{G\eta}=30000$	$K_{G\eta}=20000$	$K_{G\eta}=10000$	$K_{G\eta}=0$
0	5.11256	5.11256	5.11256	5.11256	5.11256
0.05	5.11056	5.11111	5.11245	5.11427	5.11507
0.1	5.10856	5.10966	5.11234	5.11597	5.11757
0.15	5.10656	5.10821	5.11223	5.11768	5.12008
0.2	5.10456	5.10675	5.11212	5.11938	5.12258
0.25	5.10256	5.10530	5.11201	5.12109	5.12509
0.3	5.10056	5.10385	5.11191	5.12279	5.12759
0.35	5.09856	5.10240	5.11180	5.12450	5.13010
0.4	5.09656	5.10095	5.11169	5.12620	5.13260
0.45	5.09456	5.09950	5.11158	5.12791	5.13511
0.5	5.09256	5.09804	5.11147	5.12961	5.13761
0.55	5.09056	5.09659	5.11136	5.13132	5.14012
0.6	5.08856	5.09514	5.11125	5.13302	5.14262
0.65	5.08656	5.09369	5.11114	5.13473	5.14513
0.7	5.08456	5.09224	5.11103	5.13643	5.14763
0.75	5.08256	5.09079	5.11092	5.13814	5.15014
0.8	5.08056	5.08934	5.11082	5.13984	5.15264
0.85	5.07856	5.08788	5.11071	5.14155	5.15515
0.9	5.07656	5.08643	5.11060	5.14325	5.15765
0.95	5.07456	5.08498	5.11049	5.14496	5.16016
1	5.07256	5.08353	5.11038	5.14666	5.16266
1.05	5.07056	5.08208	5.11027	5.14837	5.16517
1.1	5.06856	5.08063	5.11016	5.15007	5.16767
1.15	5.06656	5.07917	5.11005	5.15178	5.17018
1.2	5.06456	5.07772	5.10994	5.15348	5.17268
1.25	5.06256	5.07627	5.10983	5.15519	5.17519
1.3	5.06056	5.07482	5.10972	5.15689	5.17769
1.35	5.05856	5.07337	5.10962	5.15860	5.18020
1.4	5.05656	5.07192	5.10951	5.16030	5.18270
1.45	5.05456	5.07046	5.10940	5.16201	5.18521
1.5	5.05256	5.06901	5.10929	5.16371	5.18771
1.55	5.05056	5.06756	5.10918	5.16542	5.19022
1.6	5.04856	5.06611	5.10907	5.16712	5.19272
1.65	5.04656	5.06466	5.10896	5.16883	5.19523
1.7	5.04456	5.06321	5.10885	5.17053	5.19773
1.75	5.04256	5.06176	5.10874	5.17224	5.20024
1.8	5.04056	5.06030	5.10863	5.17394	5.20274
1.85	5.03856	5.05885	5.10853	5.17565	5.20525
1.9	5.03656	5.05740	5.10842	5.17735	5.20775
1.95	5.03456	5.05595	5.10831	5.17906	5.21026
2	5.03256	5.05450	5.10820	5.18076	5.21276
2.05	5.03056	5.05305	5.10809	5.18247	5.21527
2.1	5.02856	5.05159	5.10798	5.18417	5.21777
2.15	5.02656	5.05014	5.10787	5.18588	5.22028
2.2	5.02456	5.04869	5.10776	5.18758	5.22278
2.25	5.02256	5.04724	5.10765	5.18929	5.22529
2.3	5.02056	5.04579	5.10754	5.19099	5.22779
2.35	5.01856	5.04434	5.10744	5.19270	5.23030
2.4	5.01656	5.04289	5.10733	5.19440	5.23280
2.45	5.01456	5.04143	5.10722	5.19611	5.23531
2.5	5.01256	5.03998	5.10711	5.19781	5.23781

Effect of small scale parameter is studied on the bending responses of a circular micro plate. Listed in Table 8 is variation of deflection in terms of h/l.

Table 9 lists variation of deflection in terms of r/h for various h/l. An increase in thickness to micro length scale parameter h/l yields a softer micro plate with an increase in maximum deflection.

Table 10 investigates effect of n on the variation of deflection in terms of ht/h. An enhancement in deflection is observed with an increase in in-homogeneous index, n and a decrease in ht/h.

Table 11 investigates effect of spring and shear parameters of orthotropic Pasternak foundation along directions ξ and η with local angle δ on the variation of natural frequencies of microplate. Table 11 shows variation of deflection in terms of $K_{G\xi}$ for various values of $K_{G\eta}$.

5. Conclusions

In the present study, bending and free vibration analyses of a micro annular plate with piezomagnetic layers were investigated based on FSDT in the presence of magnetic field and resting on the elastic foundation. The multi-field constitutive relations are developed using modified strain gradient theory and the equilibrium governing equations of motion micro annular plate are derived using minimum of total potential energy and Hamilton's principles. One can arrive at numerical results using the semi analytical solution procedure. The Ritz method is used to obtain the results in the parametric state. The boundary conditions are applied to guess the primary functions and the minimization is used to obtain the unknown coefficients in the assumed solution. The effect of micro parameter, various geometric parameter and the foundation parameter is studied on the dynamic and static responses.

The results show an enhancement in structural stiffness of the sandwich microplate with an enhancement in the micro length scale parameter. This is according to the obtained results in the literature.

An enhancement in the natural frequencies is observe using the more stiffness foundation with an increase in three mentioned parameters.

The thickness has an increasing effect on the natural frequency as well as a decrease in bending results.

References

Adab, N., Arefi, M. and Amabili, M. (2022), "A comprehensive vibration analysis of rotating truncated sandwich conical microshells including porous core and GPL-reinforced face-sheets", *Compos. Struct.*, **279**, 114761. https://doi.org/10.1016/j.compstruct.2021.114761.

Arefi, M. (2016), "Analysis of wave in a functionally graded magneto-electro-elastic nano-rod using nonlocal elasticity model subjected to electric and magnetic potentials", *Acta. Mech.*, **227**, 2529-2542. https://doi.org/10.1007/s00707-016-1584-7.

Arefi, M. (2018), "Nonlocal free vibration analysis of a doubly curved piezoelectric nano shell", *Steel. Compos. Struct.*, **27**(4), 479-493. https://doi.org/10.12989/scs.2018.27.4.479.

Arefi, M. and Mohammad-Rezaei Bidgoli, E. (2019), "Electro-elastic displacement and stress analysis of the piezoelectric doubly curved shells resting on Winkler's foundation subjected to applied voltage", *Mech. Adv. Mater. Struct.*, **26**(23), 1981-1994. https://doi.org/10.1080/15376494.2018.1455937.

Arefi, M. and Rahimi, G.H. (2010), "Thermo elastic analysis of a functionally graded cylinder under internal pressure using first order shear deformation theory", *Sci. Res. Essays*., **5**(12), 1442–1454. https://doi.org/10.5897/SRE.9000953.

Arefi, M. and Zenkour, A.M. (2016), "Free vibration, wave propagation and tension analyses of a sandwich micro/nano rod subjected to electric potential using strain gradient theory", *Mater. Res. Exp.*, **3**(11), 115704. https://doi.org/10.1088/2053-1591/3/11/115704.

Arefi, M. and Zenkour, A.M. (2017a), "Electro-magneto-elastic analysis of a three-layer curved beam", *Smart. Struct. Syst*., **19**(6), 695-703. https://doi.org/10.12989/sss.2017.19.6.695.

Arefi, M. and Zenkour, A.M. (2017b), "Transient analysis of a three-layer microbeam subjected to electric potential", *Int. J. Smart. Nano. Mater*., **8**(1), 20-40. https://doi.org/10.1080/19475411.2017.1292967.

Arefi, M. and Zenkour, A.M. (2017c), "Thermo-electro-magneto-mechanical bending behavior of size-dependent sandwich piezomagnetic nanoplates", *Mech. Res. Commun.*, **84**, 27-42. https://doi.org/10.1016/j.mechrescom.2017.06.002.

Arefi, M., Bidgoli, E.M.R., Dimitri, R., Tornabene, F. and Reddy, J.N. (2019c), "Size-dependent free vibrations of FG polymer composite curved nanobeams reinforced with graphene nanoplatelets resting on Pasternak foundations", *Appl. Sci*., **9**(8), 1580. https://doi.org/10.3390/app9081580.

Arefi, M., Bidgoli. E.M.R. and Zenkour, A.M. (2019b), "Free vibration analysis of a sandwich nano-plate including FG core and piezoelectric face-sheets by considering neutral surface", *Mech. Adv. Mater. Struct.*, **26**(9), 741-752, https://doi.org/10.1080/15376494.2018.1455939.

Arefi, M., Faegh, R.K. and Loghman, A. (2016), "The effect of axially variable thermal and mechanical loads on the 2D thermoelastic response of FG cylindrical shell", *J. Therm. Stress.*, **39**(12), 1539-1559. https://doi.org/10.1080/01495739.2016.1217178.

Arefi, M., Lori Dehsaraji, M. and Loghman, A. (2020), "Three dimensional free vibration analysis of functionally graded nano cylindrical shell considering thickness stretching effect", *Steel. Compos. Struct*., **34**(5), 657-670. https://doi.org/10.12989/scs.2020.34.5.657.

Arefi, M., Mohammad-Rezaei Bidgoli, E. and Civalek, O. (2022), "Bending response of FG composite doubly curved nanoshells with thickness stretching via higher-order sinusoidal shear theory", *Mech. Based. Des. Struc.*, **50**(7), 2350-2378. https://doi.org/10.1080/15397734.2020.1777157.

Arefi, M., Mohammad-Rezaei Bidgoli, E. and Rabczuk, T. (2019a), "Thermo-mechanical buckling behavior of FG GNP reinforced micro plate based on MSGT", *Thin. Walled. Struct.*, **142**, 444-459. https://doi.org/10.1016/j.tws.2019.04.054.

Arefi, M., Mohammad-Rezaei Bidgoli, E. and Zenkour, A.M. (2018), "Size-dependent free vibration and dynamic analyses of a sandwich microbeam based on higher-order sinusoidal shear deformation theory and strain gradient theory", *Smart. Struct. Syst.*, **22**(1), 27-40. https://doi.org/10.12989/sss.2018.22.1.027.

Arefi, M., Rahimi, G.H. and Khoshgoftar, M.J. (2012), "Exact solution of a thick walled functionally graded piezoelectric cylinder under mechanical, thermal and electrical loads in the magnetic field", *Smart. Struct. Syst.*, **9**(5), 427-439. https://doi.org/10.12989/sss.2012.9.5.427.

Asadzadeh Khoshemehr, G. and Bahadori, H. (2023), "Investigating the dynamic response of deep soil mixing and gravel drain columns in the liquefiable layer with different thickness", *Geomech. Eng*., **34**(6), 665-681. https://doi.org/10.12989/gae.2023.34.6.665.

Bai, B. Bai, F., Li, X., Nie, Q., Jia, X. and Wu, H. (2022a), "The remediation efficiency of heavy metal pollutants in water by industrial red mud particle waste", *Environ. Technol. Innov.*, **28**, 102944. https://doi.org/10.1016/j.eti.2022.102944.

Bai, B., Bai, F., Nie, Q. and Jia, X. (2023), "A high-strength red mud–fly ash geopolymer and the implications of curing temperature". *Powder. Technol*., **416**, 118242. https://doi.org/10.1016/j.powtec.2023.118242.

Bai, B., Chen, J., Bai,F., Nie, X. and Jia, X. (2024a), "Corrosion effect of acid/alkali on cementitious red mud-fly ash materials containing heavy metal residues", *Environ. Technol. Innov.*, **33**, 103485. https://doi.org/10.1016/j.eti.2023.103485.

Bai, B., Chen, J., Zhang, B., Chen, L. and Zong, Y.(2024b), "The solidification of heavy metal Pb2+-contaminated soil by enzyme-induced calcium carbonate precipitation combined with biochar". *Biochem. Eng. J.*, **212**, 109496. https://doi.org/10.1016/j.bej.2024.109496.

Bai, B., Xu, T., Nie, Q. and Li, P. (2020), "Temperature-driven migration of heavy metal Pb2+ along with moisture movement in unsaturated soils", *Int. J. Heat. Mass. Tran*., **153**, 119573. https://doi.org/10.1016/j.ijheatmasstransfer.2020.119573.

Bai, B., Zhang, B., Chen, J. and Feng, H. (2024c), "Development of a natural inorganic diatomite curing agent on heavy metal-contaminated loess", *Phys. Chemist. Earth.*, **136**, 103790. https://doi.org/10.1016/j.pce.2024.103790.

Bai, Y., Alzahrani, B. and Baharom, S. (2022b), "Semi-numerical simulation for vibrational responses of the viscoelastic imperfect annular system with honeycomb core under residual pressure", *Eng. Comput.*, **38**(5), 3699-3724. https://doi.org/10.1007/s00366-020-01191-9.

Bao, X., Li, J., Shen, J., Chen, X., Zhang, C. and Cui, H. (2025), "Comprehensive multivariate joint distribution model for marine soft soil based on the vine copula", *Comput. Geotech*,, **177**, A, 106814. https://doi.org/10.1016/j.compgeo.2024.106814.

Chen, F., Chen, J., Duan, R., Habibi, M. and Khadimallah, M.A. (2022), "Investigation on dynamic stability and aeroelastic characteristics of composite curved pipes with any yawed angle", *Compos, Struct.*, **284**, 115195.. https://doi.org/10.1016/j.compstruct.2022.115195.

Chen, X., Feng, P. and Li, X. (2024), "High reactivity of Dimethyl ether activated by zeolite ferrierite within a fer cage: A prediction study", *Molecules*, **29**, 2000. https://doi.org/10.3390/molecules29092000.

Cui, M., Han, D., Liu, H., Li, K.C., Tang, M., Chang, C.C., Ayaz, F., Sheng, Z. and Guan, Y.L. (2024), "Secure data sharing for consortium blockchainEnabled vehicular social networks", *IEEE. T. Veh. Technol*., https://doi.org/10.1109/TVT.2024.3448207.

Dai, Z., Jiang, Z., Zhang, L. and Habibi, M. (2021), "Frequency characteristics and sensitivity analysis of a size-dependent laminated nanoshell", *Adv. Nano. Res*., **10**(2), 175-189. https://doi.org/10.12989/anr.2021.10.2.175.

Dai, Z., Wu, S., Habibi, M. and Ali, H.E. (2023), "Application of point interpolation mesh-free method for magneto/electro rheological vibrations of sandwich conical panels", *Aerosp. Sci. Technol.*, **135**, 108180. https://doi.org/10.1016/j.ast.2023.108180.

Fan, J., Pan, Y., Wang, H. and Song, F. (2024a), "Efficient reverse osmosis-based desalination using functionalized graphene oxide nanopores", *Appl. Surf. Sci.*, **674**, 160937. https://doi.org/10.1016/j.apsusc.2024.160937.

Fan, J., Zhang, X., He, N., Song, F. and Zhang, X. (2024b), "Physical absorption and thermodynamic modeling of CO2 in new deep eutectic solvents", *J. Molec. Liq.*, **402**, 124752. https://doi.org/10.1016/j.molliq.2024.124752.

Fu, T., Hu, X. and Yang, C. (2023), "Impact response analysis of stiffened sandwich functionally graded porous materials doubly-curved shell with re-entrant honeycomb auxetic core", *Appl.*

Math. Model., **124**, 553-575. https://doi.org/10.1016/j.apm.2023.08.024.

Gao, X., Dai, Y., Zhang, C. *et al*., (2023), "When it's heavier: Interfacial and solvation chemistry of isotopes in aqueous electrolytes for zn-ion batteries", *Angew. Chem. Int. Ed*., **62**(16). e202300608. https://doi.org/10.1002/anie.202300608.

Ge, J., Hong, Y., Zeng, R., Li, Y. and Habibi, M. (2023), "Increasing the attractiveness of physical education training with the involvement of nanotechnology", *Adv. Concrete Constr*., **16**(6), 291-302. https://doi.org/10.12989/acc.2024.16.6.291.

Gu, X., He, J., Wang, Z., Li, M., Habibi, M. and Hashemabadi, D. (2023), "Application of hyperbolic differential quadrature method for vibration responses of the electrorheological disk", *Eng. Anal. Bound. Elem.*, **155**, 599-615. https://doi.org/10.1016/j.enganabound.2023.05.035.

Guo, S. Deng, B., Chen, C., Ke, J., Wang, J., Long, S. and Xu. K. (2024a), "Seeking in ride-on-demand service: A reinforcement learning model with dynamic price prediction", *IEEE. Internet. Things. J.*, **11**(18), 29890-29910. https://doi.org/10.1109/JIOT.2024.3407119.

Guo, Y., Maalla, A., Habibi, M. and Moradi, Z. (2024b), "Electroelastic wave dispersion in the rotary piezoelectric NEMS sensors/actuators via nonlocal strain gradient theory", *Mech. Syst. Signal. Pr.*, **216**, 111453. https://doi.org/10.1016/j.ymssp.2024.111453.

Han, D., Pan, N. and Li, K.C. (2022a), "A traceable and revocable ciphertext-policy attribute-based encryption scheme based on privacy protection", *IEEE. Trans. Depend. Sec. Comput*., **19**(1), 316-327. https://doi.org/10.1109/TDSC.2020.2977646.

Han, D., Shi, J., Zhao, J., Wu, H., Zhou, Y., Li, L.H., Khan, M.K. and Li, K.C. (2025), "LRCN: Layer-residual co-attention networks for visual question answering", *Exp. Syst. Appl*., **263**,125658. https://doi.org/10.1016/j.eswa.2024.125658.

Han, D., Zhu, Y., Li, D., Liang, W., Souri A. and Li, K.C. (2022b), "A blockchain-based auditable access control system for Private data in service-centric IoT environments", *IEEE. T. Indust. Inform.*, **18**(5), 3530-3540. https://doi.org/10.1109/TII.2021.3114621.

Huang, B., Kang, F., Li, X. and Zhu, S. (2024a), "Underwater dam crack image generation based on unsupervised image-to-image translation", *Automat. Constr.*, **163**, 105430. https://doi.org/10.1016/j.autcon.2024.105430.

Huang, H., Xue, C., Zhang, W. and Guo, M. (2022b), "Torsion design of CFRP-CFST columns using a data-driven optimization approach", *Eng. Struct.*, **251**, 113479. https://doi.org/10.1016/j.engstruct.2021.113479.

Huang, J., Feng, C., Wang, X. and Zhang, Y. (2024b), "Continuous–discontinuous element method for simulating three-dimensional reinforced concrete structures", *Struct. Concrete*, https://doi.org/10.1002/suco.202300531

Huang, J., Pan, Z., Yang, S., Habibi, M. and Safa, M. (2024c), "Bending-based solution methodology using eigenvalue-eigenvector approach for analysis of foldable reinforced Golf Clubs cylindrical shell", *Mech. Adv. Mater. Struct*., https://doi.org/10.1080/15376494.2024.2378372.

Huang, X., Chang, L., Zhao, H. and Cai, Z. (2022a), "Study on craniocerebral dynamics response and helmet protective performance under the blast waves", *Mater. Design*, **224**, 111408. https://doi.org/10.1016/j.matdes.2022.111408.

Huo, J., Zhang, G., Ghabussi, A. and Habibi, M. (2021), "Bending analysis of FG-GPLRC axisymmetric circular/annular sector plates by considering elastic foundation and horizontal friction force using 3D-poroelasticity theory", *Compos. Struct.*, **276**, 114438. https://doi.org/10.1016/j.compstruct.2021.114438.

Jaber, L., Mezeh, R., Zein, Z., Azab, M. and Sadek, M. (2023), "Nonlinear numerical analysis of influence of pile inclination on the seismic response of soil-pile-structure system", *Geomech. Eng.*, **34**(4), 437-447. https://doi.org/10.12989/gae.2023.34.4.437.

Jafarsadeghi-pournaki, I., Fakhari, M., Amiri, A. and Rezazadeh, G. (2015), "Vibration analysis of circular magneto-electro-Elastic Nano-plates Based on Eringen s Nonlocal Theory", *Int. J. Eng., Trans. C,* **28**(12), 1808-1817. https://doi.org/10.5829/idosi.ije.2015.28.12c.15.

Jermsittiparsert, K., Ghabussi, A., Forooghi, A., Shavalipour, A., Habibi, M., Jung, D.W. and Safa, M. (2020), "Critical voltage, thermal buckling and frequency characteristics of a thermally affected GPL reinforced composite microdisk covered with piezoelectric actuator", *Mech. Based. Des. Struc*., **50**(4), 1331-1353. https://doi.org/10.1080/15397734.2020.1748052.

Ji, X., Jiang, P., Jiang, Y., Chen, H. and Wang, W. (2023), "Toward enhanced aerosol particle adsorption in never-bursting bubble via acoustic levitation and controlled liquid compensation", *Adv. Sci.*, **10**(19), 2300049. https://doi.org/10.1002/advs.202300049.

Jin, Z., Huo, W., Habibi, M. and Albaijan, I. (2024), "Thermo-foldable bending analysis of tunable shells using a higher-order modeling", *Mech. Adv. Mater. Struct*., https://doi.org/10.1080/15376494.2024.2369263.

Kandaz, M. and Dal, H. (2021), "Finite element analyses of the modified strain gradient theory based kirchhoff microplates", *Surfaces*, **4**, 115-156. https://doi.org/10.3390/surfaces4020014.

Ke. L.L., Yang, J., Kitipornchai, S. and Bradford. M.A. (2012), "Bending, buckling and vibration of size-dependent functionally graded annular micro plate", *Compos. Struct*., **94**, 3250-3257. https://doi.org/10.1016/j.compstruct.2012.04.037.

Korayem, M.H., Homayooni, A. and Sadeghzadeh, S. (2013), "Semi-analytic actuating and sensing in regular and irregular MEMs, single and assembled micro cantilevers", *Appl. Math. Model*., **37**(7), 4717-4732. https://doi.org/10.1016/j.apm.2012.09.064.

Lai, Y., Zhang, T., Yin, X., Zhu, C., Du, Y., Li, Z. and Gao, J. (2024), "An antibiotic-free platform for eliminating persistent Helicobacter pylori infection without disrupting gut microbiota", *Acta. Pharmac. Sin. B*., **14**(7), 3184-3204. https://doi.org/10.1016/j.apsb.2024.03.014.

Li, F., Gan, J., Zhang, L., Tan, H., Li, E. and Li, B. (2024e), "Enhancing impact resistance of hybrid structures designed with triply periodic minimal surfaces", *Compos. Sci. Tech*., **245**, 110365. https://doi.org/10.1016/j.compscitech.2023.110365.

Li, J. Yang, H. Gu, X. Zou, Y. Zhan D. Peng, J. (2024c), "Recent advances in scanning electrochemical microscopy for probing the sites in electrocatalysts, *J. Mater. Chem. A.* **12**. 30. 18733-18750, http://dx.doi.org/10.1039/D4TA01292E

Li, J., Han, D. and Weng, T.H. (2025), "A secure data storage and sharing scheme for port supply chain based on blockchain and dynamic searchable encryption", *Comput. Stand. Inter*., **91**, 103887. https://doi.org/10.1016/j.csi.2024.103887.

Li, J., Wu, X. and Wu, L. (2024f), "A computationally-efficient analytical model for SPM machines considering PM shaping and property distribution", *IEEE. T. Energ. Conver*., **39**(2), 1034-1046. https://doi.org/10.1109/TEC.2024.3352577.

Li, J., Wu, Z., Habibi, M. and Albaijan, I. (2024d), "An inspection of the metal-foam beam considering torsional dynamic responses", *Solid. State. Commun.*, **391**, 115638. https://doi.org/10.1016/j.ssc.2024.115638.

Li, Y., Li, J., Feng, C., Wen, M. and Zhang, Y. (2024a), "An interface constitutive model of plastic tensile–compressive damage under impact loading based on continuous–discontinuous framework", *Comput. Geotech.*, **173**, 106502. https://doi.org/10.1016/j.compgeo.2024.106502.

Li, Y., Li, S., Guo, K., Fang, X. and Habibi, M. (2022), "On the modeling of bending responses of graphene-reinforced higher

order annular plate via two-dimensional continuum mechanics approach", *Eng. Comput.*, **38**(1), 703-724. https://doi.org/10.1007/s00366-020-01166-w.

Li, Y.S., Feng, W.J. and Cai, Z.Y. (2014), "Bending and free vibration of functionally graded piezoelectric beam based on modified strain gradient theory", *Compos. Struct.*, **115**, 41-50. https://doi.org/10.1016/j.compstruct.2014.04.005.

Li, Y. Li, J. Feng, C. Wen, M. Zhang, Y. (2024b), "An interface constitutive model of plastic tensile–compressive damage under impact loading based on continuous–discontinuous framework", *Comput. Geotech.*, **173**, 106502. https://doi.org/10.1016/j.compgeo.2024.106502

Liang, Z., Zhao, Y., Yu, H., Habibi, M. and Mahmoudi, T. (2024), "Artificial neural networks coupled with numerical approach for the stability prediction of non-uniform functionally graded microscale cylindrical structures", *Structures*, **60**, 105826. https://doi.org/10.1016/j.istruc.2023.105826.

Liew, K.M., Wang, C.M., Xiang, Y. and Kitipornchai, S. (1998), "Vibration of Mindlin plates: Programming the p-version Ritz method", Oxford: Elsevier Science, https://doi.org/10.1016/B978-0-08-043341-7.X5000-6

Liu, H., Zhang, Q., Yang, X. and Ma, J. (2021), "Size-dependent vibration of laminated composite nanoplate with piezo-magnetic face sheets", *Eng. Comput*., https://doi.org/10.1007/s00366-021-01285-y.

Liu, H., Zhao, Y., Pishbin, M., Habibi, M., Bashir, M.O. and Issakhov, A. (2022), "A comprehensive mathematical simulation of the composite size-dependent rotary 3D microsystem via two-dimensional generalized differential quadrature method". *Eng. Comput*., **38**(5), 4181-4196. https://doi.org/10.1007/s00366-021-01419-2.

Lu, K. (2024), "Online distributed algorithms for online noncooperative games with stochastic cost functions: High probability bound of regrets", *IEEE. T. Automat. Contr.*, https://doi.org/10.1109/TAC.2024.3419018.

Lu, L., Liao, K., Habibi, M., Safarpour, H. and Elhosiny Ali, H. (2023), "Numerical methods to predict aero thermally induced vibrations of a curved pipe structure reinforced by GPLs", *Structures*, **55**, 1607-1621. https://doi.org/10.1016/j.istruc.2023.06.105.

Luo, Y., Zhang, H., Chen, Z., Li, Q., Ye, S. and Liu, Q. (2024b), "Novel multidimensional composite development for aging resistance of SBS-Modified asphalt by attaching zinc oxide on expanded vermiculite", *Energ.. Fuel.*, **38**(17), 16772-16781. https://doi.org/10.1021/acs.energyfuels.4c02685.

Luo, Y.X. and Dong, Y.L. (2024a), "Strain measurement at up to 3000°C based on ultraviolet-digital image correlation", *NDT & E Int.*, **146**, 103155. https://doi.org/10.1016/j.ndteint.2024.103155.

Lv, H., Zeng, J., Zhu, Z., Dong, S. and Li, W. (2024), "Study on prestress distribution and structural performance of heptagonal six-five-strut alternated cable dome with inner hole", *Structures*, **65**, 106724. https://doi.org/10.1016/j.istruc.2024.106724.

Ma, B., Chen, K.Y., Habibi, M. and Albaijan, I. (2023), "Static/dynamic analyses of sandwich micro-plate based on modified strain gradient theory", *Mech. Adv. Mater. Struct*., https://doi.org/10.1080/15376494.2023.2219453.

Meng, F., Pang, A., Dong, X., Han, C. and Sha, X. (2018), "H∞ optimal performance design of an unstable plant under bode integral constraint", *Complexity*, https://doi.org/10.1155/2018/4942906.

Meng, F., Wang, D., Yang, P. and Xie, G. (2019), "Application of sum of squares method in nonlinear H∞ control for satellite attitude maneuvers", *Complexity*, https://doi.org/10.1155/2019/5124108.

Meng, S., Meng, F., Chi, H., Chen, H. and Pang, A. (2023), "A robust observer based on the nonlinear descriptor systems application to estimate the state of charge of lithium-ion batteries", *J. Frank. Inst.*, **360**(16), 11397-11413. https://doi.org/10.1016/j.jfranklin.2023.08.037.

Meng, S., Meng, F., Zhang, F., Li, Q., Zhang, Y. and Zemouche, A. (2024), "Observer design method for nonlinear generalized systems with nonlinear algebraic constraints with applications", *Automatica*, **162**, 111512. https://doi.org/10.1016/j.automatica.2024.111512.

Mohammad-Rezaei Bidgoli E. and Arefi. M. (2023b), "Dynamic results of GNPRC sandwich shells", *Steel. Compos. Struct.*, **48**(3), 263-273. https://doi.org/10.12989/scs.2023.48.3.263.

Mohammad-Rezaei Bidgoli, E. and Arefi, M. (2021), "Free vibration analysis of micro plate reinforced with functionally graded graphene nanoplatelets based on modified strain-gradient formulation", *J. Sandw. Struct. Mater.*, **23**(2), 436-472. https://doi.org/10.1177/1099636219839302.

Mohammad-Rezaei Bidgoli, E. and Arefi, M. (2022), "Innovations in graphene-based polymer composites", Woodhead Publishing Series in Composites Science and Engineering, 521-557. https://doi.org/10.1016/B978-0-12-823789-2.00003-0.

Mohammad-Rezaei Bidgoli, E. and Arefi, M. (2023a), "Size-dependent thermomechanical critical loads of GPL-reinforced nanobeams", *Wave. Random. Complx*, 1-21. https://doi.org/10.1080/17455030.2023.2169385.

Mohammad-Rezaei Bidgoli, E. and Arefi, M. (2023c), "Effect of porosity and characteristics of carbon nanotube on the nonlinear characteristics of a simply-supported sandwich plate", *Archiv. Civ. Mech. Eng*., **23**, 214. https://doi.org/10.1007/s43452-023-00752-1.

Mohammad-Rezaei Bidgoli, E. and Arefi, M. (2023d), "Nonlinear vibration analysis of sandwich plates with honeycomb core and graphene nanoplatelet-reinforced face-sheets", *Archiv. Civ. Mech. Eng.*, **23**, 56. https://doi.org/10.1007/s43452-022-00589-0.

Peng, S., Habibi, M. and Pourjabari, A. (2023), "Generalized differential quadrature element solution, swarm, and GA optimization technique to obtain the optimum frequency of the laminated rotary nanostructure", *Eng. Anal. Bound. Elem.*, **151**, 101-114. https://doi.org/10.1016/j.enganabound.2023.02.052.

Pi, X., Yan, D., Xu, Y., Pan, M., Wang, Z., Chang, M. and Qi, Z. (2025), "TLRs signaling pathway regulation, antibacterial and apoptotic activity of largemouth bass ECSIT during Edwardsiella piscicida infection", *Aquaculture*, **595**(2), 741615. https://doi.org/10.1016/j.aquaculture.2024.741615.

Prasad, S.A.N., Gallas, Q., Horowitz, S., Homeijer, B., Sankar, B. V., Cattafesta, L.N. and Sheplak, M. (2006), "Analytical electroacoustic model of a piezoelectric composite circular plate", *AIAA J.*, **44**(10). https://doi.org/10.2514/1.19855.

Ren, H., Xia, X., Sun, Y., Zhai, Y., Zhang, Z., Wu, J., Li, J. and Liu, M. (2024), "Electrolyte engineering for the mass exfoliation of graphene oxide across wide oxidation degrees". *J. Mater. Chem. A.*, **12**(35), 23416-23424. https://doi.org/10.1039/D4TA02654C.

Sadeghzadeh, S. and Kabiri, A. (2017), "A hybrid solution for analyzing nonlinear dynamics of electrostatically-actuated microcantilevers", *Appl. Math. Model.,* **48**, 593-606. https://doi.org/10.1016/j.apm.2017.04.017.

Sarvesh, R., Srinivasan, V. and Patel, A. (2023), "Finite element limit analysis of the bearing capacity of an obliquely loaded strip footing on granular soil placed adjacent to vertically loaded existing footing", *Geomech. Eng.*, **35**(3), 287-306. https://doi.org/10.12989/gae.2023.35.3.

Shi, J., Han, D., Chen, C. and Shen, X. (2024), "KTMN: Knowledge-driven Two-stage Modulation Network for visual question answering", *Multimed. Syst.*, **30**, 350. https://doi.org/10.1007/s00530-024-01568-6.

Shi, X., Li, J. and Habibi, M. (2022), "On the statics and dynamics of an electro-thermo-mechanically porous GPLRC nanoshell conveying fluid flow", *Mech. Based. Des. Struc.*, **50**(6), 2147-2183. https://doi.org/10.1080/15397734.2020.1772088.

Shin, H. (2023), "Static and quasi-static slope stability analyses using the limit equilibrium method for mountainous area", *Geomech. Eng.*, **34**(2), 187-195. https://doi.org/10.12989/gae.2023.34.2.187.

Song, G., Zou, Y., Nie, Y., Habibi, M., Albaijan, I. and Toghroli, E. (2024b), "Application of Hashin–Shtrikman bounds homogenization model for frequency analysis of imperfect FG bio-composite plates", *J. Mech. Beh. Biomed. Mater.*, **151**, 106321. https://doi.org/10.1016/j.jmbbm.2023.106321.

Song, X., Han, D., Chen, C., Shen, X. and Wu, H. (2024a), "Vman: visual-modified attention network for multimodal paradigms", *Vis Comput.*, https://doi.org/10.1007/s00371-024-03563-4.

Su, Y., Zhu, J., Long, X., Zhao, L., Chen, C. and Liu, C. (2023), "Statistical effects of pore features on mechanical properties and fracture behaviors of heterogeneous random porous materials by phase-field modeling", *Int. J. Solids. Struct.*, **264**, 112098. https://doi.org/10.1016/j.ijsolstr.2022.112098.

Sun, L., Wei, C., Liu, F., Wang, L. and Ren, B. (2023), "On the wave propagations of football game ball after contacting with the player foot", *Geomech. Eng.*, **33**(6), 529-542. https://doi.org/10.12989/gae.2023.33.6.529.

Sun, X., Zhang, K., Liu, Q., Bao, M. and Chen, Y. (2024), "Harnessing domain insights: A prompt knowledge tuning method for aspect-based sentiment analysis", *Know. Based. Syst.*, **298**, 111975. https://doi.org/10.1016/j.knosys.2024.111975.

Thai, S., Thai, H.T. Vo, T.P. and Patel, V.I. (2017), "Size-dependant behaviour of functionally graded microplates based on the modified strain gradient elasticity theory and isogeometric analysis", *Comput. Struct.*, **190**, 219-241. https://doi.org/10.1016/j.compstruc.2017.05.014.

Wang, C., Habibi, M. and Mahmoudi, T. (2024d), "Stability analysis of the nonuniform functionally graded cylindrical small-scale beam structures: Application in sport structures", *Steel. Compos. Struct.* **52**(1), 15-29. https://doi.org/10.12989/scs.2024.52.1.015.

Wang, C., Song, Z. and Fan, H. (2024f), "Novel evidence theory-based reliability analysis of functionally graded plate considering thermal stress behavior", *Aerosp. Sci. Technol*., **146**, 108936. https://doi.org/10.1016/j.ast.2024.108936.

Wang, C., Yang, L., Hu, M., Wang, Y. and Zhao, Z. (2024c), "On-demand airport slot management: tree-structured capacity profile and coadapted fire-break setting and slot allocation", *Transportmetrica A: Transport Sci*., 1-35. https://doi.org/10.1080/23249935.2024.2393224.

Wang, R., Han, Q. and Pan, E. (2010), "An analytical solution for a multilayered magneto-electro-elastic circular plate under simply supported lateral boundary conditions", *Smart. Mater. Struct.,* **19**(6). https://doi.org/10.1088/0964-1726/19/6/065025.

Wang, S., He, J., Fan, J., Sun, P. and Wang, D. (2023b), "A time-domain method for free vibration responses of an equivalent viscous damped system based on a complex damping model", *J. Low. Frequency. Noise. Vib. Active. Cont*., **42**(3), 1531-1540. https://doi.org/10.1177/14613484231157514.

Wang, W., Zhang, J., Habibi, M. and Albaijan, I. (2024e), "Stretchable-thickness model for dynamic responses of graphene origami reinforced badminton sport plate", *Mech. Adv. Mater. Struct*., https://doi.org/10.1080/15376494.2024.2373976

Wang, Y., Jia, Q., Deng, T., Habibi, M., Al-Kikani, S. and Ali, H.E. (2023c), "Wave propagation analysis of the ball in the handball's game", *Struct. Eng. Mech.*, **85**(6), 729-742. https://doi.org/10.12989/sem.2023.85.6.729.

Wang, Y., Wang, J., Cai, R., Zhang, J., Xia, S., Li, Z., Yu, C., Wu, J., Wang, P. and Wu, y. (2024a), "Enhanced local CO coverage on Cu quantum dots for boosting electrocatalytic CO_2 reduction to ethylene", *Adv. Funct. Mater*., https://doi.org/10.1002/adfm.202417764.

Wang, Z., Liao, Z., Zhou, B., Yu G. and Luo, W. (2024b), "SwinURNet: Hybrid transformer-CNN architecture for real-time unstructured road segmentation", *IEEE. T. Instrum. Meas.*, **73**, 1-16. 5035816, https://doi.org/10.1109/TIM.2024.3470042.

Wang, Z., Wang, S., Wang, X. and Luo, X. (2023a), "Permanent magnet-based superficial flow velometer with ultralow output drift", *IEEE. T. Instrum. Meas*., **72**, 1-12. https://doi.org/10.1109/TIM.2023.3304692.

Wu, J. and Habibi, M. (2022), "Dynamic simulation of the ultra-fast-rotating sandwich cantilever disk via finite element and semi-numerical methods", *Eng. Comput.*, **38**(5), 4127-4143. https://doi.org/10.1007/s00366-021-01396-6.

Wu, Y., Kang, F., Zhang, Y., Li, X. and Li, H. (2024), "Structural identification of concrete dams with ambient vibration based on surrogate-assisted multi-objective salp swarm algorithm", *Structures*, **60**, 105956. https://doi.org/10.1016/j.istruc.2024.105956

Xiao, H., Habibi, M. and Habibi, M. (2024), "Bulk wave propagation analysis of imperfect FG bio-composite beams resting on variable elastic medium", *Mater. Today. Commun.*, https://doi.org/10.1016/j.mtcomm.2024.108524.

Xiao, Z.Y., Li, Y.J., Zhang, W. *et al*. (2022), "Enhancement of torque efficiency and spin Hall angle driven collaboratively by orbital torque and spin–orbit torque", *Appl. Phys. Lett.*, **121**(7), 072404. https://doi.org/10.1063/5.0086125.

Xie, J., Wen, M., Ding, P., Tu, Y., Wu, D., Liu, K., Tang, K. and Chen, M. (2024a), "Interfacial flow contact resistance effect for thermal consolidation of layered viscoelastic saturated soils with semi-permeable boundaries", *Int. J. Num. Anal. Meth. Geomech*., **48**(15), 3640-3679. https://doi.org/10.1002/nag.3805.

Xie, J., Wen, M., Tu, Y., Wu, D., Liu, K. and Tang, K. (2024b), "Thermal consolidation of layered saturated soil under time-dependent loadings and heating considering interfacial flow contact resistance effect", *Int. J. Num. Anal. Meth. Geomech*., **48**(5), 1123-1159. https://doi.org/10.1002/nag.3677.

Xin, J., Xu, W., Cao, B., Wang, T. and Zhang, S. (2024), "A deep-learning-based MAC for integrating channel access, rate adaptation and channel switch", *Comput. Sci., Netw. Internet. Arch.*, https://doi.org/10.48550/arXiv.2406.02291.

Xu, C., Zhu, M., Wang, Q., *et al*. (2023), "TROP2-directed nanobody-drug conjugate elicited potent antitumor effect in pancreatic cancer", *J. Nanobiotech.*, **21**, 410. https://doi.org/10.1186/s12951-023-02183-9.

Yan, C., Feng, M., Wu, Z., Guo, Y., Dong, W., Wang, Y. and Mian, A. (2024), "Discriminative correspondence estimation for unsupervised RGB-D point cloud registration", *IEEE. T. Circ. Syst. Video. Tech.*, https://doi.org/10.1109/TCSVT.2024.3480268.

Yin, J., Zou, Y., Li, J., Zhang, W., Li, and Habibi, M. (2024), "Dynamic stability and frequency responses of the tilted curved nanopipes in a supersonic airflow via 2D hybrid nonlocal strain gradient theory", *Eng. Struct.*, **301**, 117240.. https://doi.org/10.1016/j.engstruct.2023.117240.

Yu, C., Lin, P., Wu, Z., Habibi, M. and Zhang, W. (2024), "Multi-load effect on the deformation analysis of composite nano reinforced origami sandwich panel", *Mech. Adv. Mater. Struct*., 1-19. https://doi.org/10.1080/15376494.2024.2367015.

Yu, L,, Lei, Y,, Ma, Y,, Liu, M,, Zheng, J,, Dan, D. and Gao, P. (2021), "A comprehensive review of fluorescence correlation spectroscopy", *Front. Phys.*, **9**, 644450. https://doi.org/10.3389/fphy.2021.644450.

Yuan, X., Wang, W., Pang, H. and Zhang, L. (2024), "Analysis of vibration characteristics of electro-hydraulic driven 3-UPS/S parallel stabilization platform", *Chin. J. Mech. Eng*., **37**(1), 96. https://doi.org/10.1186/s10033-024-01074-w.

Zhang, C., Khorshidi, H., Najafi, E. and Ghasemi, M. (2023e), "Fresh, mechanical and microstructural properties of alkali-activated composites incorporating nanomaterials: A comprehensive review". *J. Cleaner. Prod.*, **384**, 135390. https://doi.org/10.1016/j.jclepro.2022.135390.

Zhang, D., Huang, X., Wang, T., Habibi, M., Albaijan, I. and Toghroli, E. (2024e), "Dynamic stability improvement in spinning FG-piezo cylindrical structure using PSO-ANN and firefly optimization algorithm", *Mater. Sci. Eng. B*, **302**, 117210. https://doi.org/10.1016/j.mseb.2024.117210.

Zhang, H.H., Chao, J.B., Wang, Y.W., Liu, Y., Yao, H.M., Zhao, Z.P. and Niu, K. (2024d), "5G base station antenna array with heatsink radome", *IEEE T. Antenn. Propag*., **72**(3), 2270-2278. https://doi.org/10.1109/TAP.2024.3358378.

Zhang, K., Ye, Z., Qi, M., Cai, W., Saraiva, J.L., Wen, Y., Liu, G., Zhu, Z., Zhu, S. and Zhao, J. (2024a), "Water quality impact on fish behavior: A review from an aquaculture perspective", *Rev. Aquaculture*. https://doi.org/10.1111/raq.12985.

Zhang, L., Chen, Z., Habibi, M., Ghabussi, A. and Alyousef, R. (2021c), "Low-velocity impact, resonance, and frequency responses of FG-GPLRC viscoelastic doubly curved panel", *Compos. Struct.*, **269**, 114000. https://doi.org/10.1016/j.compstruct.2021.114000.

Zhang, M., Jiang, X. and Arefi, M. (2023b), "Dynamic formulation of a sandwich microshell considering modified couple stress and thickness-stretching", *Eur. Phys. J. Plus*, **138**, 227. https://doi.org/10.1140/epjp/s13360-023-03753-4.

Zhang, Q., Xie, M., Zhou, D., Habibi, M. and Khorami, M. (2024f), "Bending responses of graphene nanoplatelets reinforced sandwich cylindrical micro panel with piezoelectric layers", *Mech. Adv. Mater. Struct.*, https://doi.org/10.1080/15376494.2024.2385008.

Zhang, Q., Zou, X., Wang, Y. and Habibi, M. (2023c), "Study on photocatalytic, electric, and sensing behavior of Co- and Ag-codoped tin dioxide (SnO2) nano particles", *Mater. Sci. Eng. B*, **296**, 116687. https://doi.org/10.1016/j.mseb.2023.116687.

Zhang, T., Xu S. and Zhang, W. (2024c), "New approach to feedback stabilization of linear discrete time-varying stochastic systems", *IEEE. Trans. Auto. Cont.*, https://doi.org/10.1109/TAC.2024.3482119.

Zhang, W., Huang, J., Lin, J., Lin, B., Yang, X. and Huan, Y. (2024g), "Experimental and numerical investigation of mechanical behavior of segmental joint of shield tunneling strengthened by prestressed CFRP plates", *Structures*, **70**, 107634. https://doi.org/10.1016/j.istruc.2024.107634.

Zhang, W., Kang, S., Liu, X., Lin, B. and Huang, Y. (2023d), "Experimental study of a composite beam externally bonded with a carbon fiber-reinforced plastic plate". *J. Build. Eng*., **71**, 106522. https://doi.org/10.1016/j.jobe.2023.106522.

Zhang, X., Chen, H., Wang, Y. Gao, X., Wang, Z., Wang, N. and Zang, D. (2024b), "Ultrasound induced grain refinement of crystallization in evaporative saline droplets", *Ultrason. Sonochem.*, **107**, 106938. https://doi.org/10.1016/j.ultsonch.2024.106938.

Zhang, Y. (2017), "Multi-slicing strategy for the three-dimensional discontinuity layout optimization (3D DLO)", *Int. J. Numer. Anal. Meth. Geomech*., **41**(4), 488-507. https://doi.org/10.1002/nag.2566.

Zhang, Y. and Mang, H.A. (2020), "Global cracking elements: A novel tool for Galerkin-based approaches simulating quasi-brittle fracture", *Int. J. Numer. Meth. Eng*., **121**(11), 2462-2480. https://doi.org/10.1002/nme.6315.

Zhang, Y. and Zhuang, X. (2018a), "A softening-healing law for self-healing quasi-brittle materials: Analyzing with strong discontinuity embedded approach", *Eng. Fract. Mech.*, **192**, 290-306. https://doi.org/10.1016/j.engfracmech.2017.12.018.

Zhang, Y. and Zhuang, X. (2018b), "Cracking elements: A self-propagating strong discontinuity embedded approach for quasi-brittle fracture", *Finite. Elem. Anal. Des.*, **144**, 84-100. https://doi.org/10.1016/j.finel.2017.10.007.

Zhang, Y. and Zhuang, X. (2019), "Cracking elements method for dynamic brittle fracture", *Theor. Appl. Fract. Mech.*, **102**, 1-9. https://doi.org/10.1016/j.tafmec.2018.09.015.

Zhang, Y., Gao, Z., Li, Y. and Zhuang, X. (2020), "On the crack opening and energy dissipation in a continuum based disconnected crack model", *Finite. Elem. Anal. Des.*, **170**, 103333. https://doi.org/10.1016/j.finel.2019.103333.

Zhang, Y., Gao, Z., Wang, X. and Liu, Q. (2022a), "Predicting the pore-pressure and temperature of fire-loaded concrete by a hybrid neural network", *Int. J. Comput. Meth.*, **19**(8), 2142011. https://doi.org/10.1142/S0219876221420111.

Zhang, Y., Gao, Z., Wang, X. and Liu, Q. (2023a), "Image representations of numerical simulations for training neural networks", *Comput. Model. Eng. Sci*., **134**(2), 821-833. https://doi.org/10.32604/cmes.2022.022088.

Zhang, Y., Huang, J., Yuan, Y. and Mang, H.A. (2021b), "Cracking elements method with a dissipation-based arc-length approach", *Finite. Elem. Anal. Des.*, **195**, 103573. https://doi.org/10.1016/j.finel.2021.103573.

Zhang, Y., Lackner, R., Zeiml, M. and Mang, H.A. (2015), "Strong discontinuity embedded approach with standard SOS formulation: Element formulation, energy-based crack-tracking strategy, and validations", *Comput. Meth. Appl. M.*, **287**, 335-366. https://doi.org/10.1016/j.cma.2015.02.001.

Zhang, Y., Wang, X., Wang, X. and Mang, H.A. (2022b), "Virtual displacement based discontinuity layout optimization". *Int. J. Numer. Meth. Eng*., **123**(22), 5682-5694. https://doi.org/10.1002/nme.7084.

Zhang, Y., Yang, X., Wang, X. and Zhuang, X. (2021a), "A micropolar peridynamic model with non-uniform horizon for static damage of solids considering different nonlocal enhancements", *Theor. Appl. Fract. Mech.*, **113**, 102930. https://doi.org/10.1016/j.tafmec.2021.102930.

Zhang, Y., Zeiml, M., Pichler, C. and Lackner, R. (2014), "Model-based risk assessment of concrete spalling in tunnel linings under fire loading", *Eng. Struct.*, **77**, 207-215. https://doi.org/10.1016/j.engstruct.2014.02.033.

Zhang, Y., Zhuang, X. and Lackner, R. (2018), "Stability analysis of shotcrete supported crown of NATM tunnels with discontinuity layout optimization", *Int. J. Numer. Anal. Meth. Geomech*., **42**(11), 1199-1216. https://doi.org/10.1002/nag.2775.

Zhao, Z., Zhang, H., Shiau, J., Du, W., Ke, L., Wu, F. and Bao, X. (2024), "Failure envelopes of rigid tripod pile foundation under combined vertical-horizontal-moment loadings in clay", *Appl. Ocean. Res.*, **150**, 104131. https://doi.org/10.1016/j.apor.2024.104131.

Zhiqiang, S., Aiyun, L., Daichang, Z., Shuangjun, L., Habibi, M., Xiaoling, F. and Albaijan, I. (2024), "Application of a folded nanostructure reinforcement for the pole vault curved shell", *Mech. Adv. Mater. Struct.*, https://doi.org/10.1080/15376494.2024.2375368

Zhu, L., Ren, H., Habibi, M., Mohammed, K.J. and Khadimallah, M.A. (2022), "Predicting the environmental economic dispatch problem for reducing waste nonrenewable materials via an innovative constraint multi-objective chimp optimization algorithm", *J. Clean. Prod.*, **365**, 132697. https://doi.org/10.1016/j.jclepro.2022.132697.